A single N6-methyladenosine site in lncRNA HOTAIR regulates its function in breast cancer cells

Authors: Allison M Porman[1], Justin T Roberts[1,2], Madeline Chrupcala[1,3], Michelle Kennedy[1], Michelle M. Williams[4], Jennifer K. Richer[4], Aaron M. Johnson[1,2,3,*]

Affiliations: [1]University of Colorado Anschutz Medical Campus, Biochemistry and Molecular Genetics Department; [2]University of Colorado Anschutz Medical Campus, Molecular Biology Graduate Program, [3]University of Colorado Anschutz Medical Campus, RNA Bioscience Initiative [4]Department of Pathology, University of Colorado Anschutz Medical Campus Aurora, Colorado.

*Corresponding Author

Aaron M. Johnson, PhD

e-mail: Aaron.m.johnson@CUAnschutz.edu

Tel: +1(303)724-3224

Abstract

N6-methyladenosine (m6A) is one of the most abundant RNA modifications with important roles in normal and cancer biology, but knowledge of its function on long noncoding RNAs (lncRNAs) remains limited. In this study, we investigate whether m6A plays a role in regulating the function of the HOTAIR lncRNA which contributes to multiple pro-tumor phenotypes in triple-negative breast cancer (TNBC) cells. We identify 14 individual m6A sites within HOTAIR, with a single site (A783) being consistently methylated. Mutation of A783 impairs cellular proliferation and colony formation in TNBC cells. We find that HOTAIR interacts with the nuclear m6A reader YTHDC1 at methylated A783 and additional sites. Interestingly, we determine that modifications at different sites in HOTAIR have differential effects on HOTAIR regulation. Specifically, m6A at A783 regulates HOTAIR localization to chromatin, whereas other m6A sites mediate high HOTAIR levels. We further find that YTHDC1-HOTAIR interactions are required for gene repression, independent of expression level and chromatin recruitment. Altogether, our work suggests a mechanism whereby m6A regulates the function of HOTAIR via mediating the interaction of YTHDC1 with specific m6A sites, promoting chromatin-mediated repression and breast cancer cell aggressiveness.

Introduction

Long non-coding RNAs (lncRNAs) are becoming increasingly noted for their roles in transcriptional regulation[1]. LncRNAs are longer than 200 nucleotides, transcribed by RNA polymerase II, and processed similarly to mRNAs[2]. LncRNAs are capable of regulating transcription in a variety of ways; they can act as chromatin regulators, directing histone-modifying enzymes to their target genes to induce changes in chromatin, or can interact with transcription factors and RNA polymerase II[1]. LncRNAs have been demonstrated to be key regulators of epigenetic changes that can drive cancer progression, often by aberrant overexpression[3].

The function of the N6-methyladenosine (m6A) RNA modification has been well studied in messenger RNAs (mRNAs), where it can regulate multiple steps of the mRNA life cycle, including processing, decay, and translation[4]. The function of m6A in lncRNA-mediated processes has only recently been studied and is less understood. For example, the lncRNA Xist, a key mediator of X chromosome inactivation during development, contains multiple m6A sites that contribute to its ability to induce repression of the X chromosome[5,6].

The m6A modification on an RNA is typically recognized by a “reader” protein that binds specifically to methylated adenosine and then acts directly or recruits other factors to mediate the functional outcome of m6A deposition. Apart from the YTH family of proteins that directly read m6A, a handful of non-canonical indirect m6A readers have been suggested[7]. In the case of Xist, the m6A reader YTHDC1 interacts with Xist to mediate repression; however, it is still unclear mechanistically how m6A and YTHDC1 contribute to repression by Xist[6,8]. In contrast, m6A on chromatin-associated regulatory RNAs leads to their YTHDC1-dependent degradation, preventing transcription of downstream genes[9]. As with m6A function in mRNAs, the context of noncoding RNA m6A methylation also dictates the functional outcome[10].

The human lncRNA HOTAIR is a 2.2kb spliced and polyadenylated RNA transcribed from the HoxC locus. Originally identified as a developmental regulator acting as a gene repressor of the HoxD locus in *trans*[11], aberrantly high expression of HOTAIR is also associated with poor survival and increased cancer properties in many different cancer types, including breast cancer[3,12]. HOTAIR mediates histone modification by Polycomb Repressive Complex 2 (PRC2) at its target genes, resulting in heterochromatin formation and repression[12–14]. In cancer contexts, high levels of HOTAIR misdirect this mechanism to genes that should not be repressed in the tissue of origin[3,15]. A recent study demonstrated that HOTAIR can repress genes even in the absence of PRC2, suggesting that initial repression or transcriptional interference may occur upstream of H3K27 trimethylation (H3K27me3) by PRC2[16] (Figure 1A). Underscoring the potential importance of this PRC2-independent pathway is the observation that RNA binding to PRC2 inhibits its

enzymatic activity[17–19]. This is confounding given that there is a massive upregulation of HOTAIR in many cancers[15]. How HOTAIR accomplishes transcriptional repression and how other pathways and cancer contexts influence HOTAIR function remains elusive.

A recent clue for additional players in lncRNA mechanisms comes from RNA modifications such as m6A which have been shown to play critical roles in several human cancers[20]. In breast cancer, recent studies have revealed that dysregulation of m6A levels can generate breast cancer stem-like cells and promote metastasis[21–23]. Of the currently designated m6A reader proteins, we have previously shown that hnRNP A2/B1, a proposed non-canonical reader lacking the m6A-binding YTH domain, can interact with HOTAIR to regulate its chromatin and cancer biology mechanisms by promoting HOTAIR interactions with target mRNAs[24]. This evidence suggests that m6A may play a role in cancers where HOTAIR is overexpressed.

Here, we set out to investigate the potential function of m6A in HOTAIR-mediated breast cancer aggressiveness. We identify 14 m6A sites in HOTAIR and show that a single site (A783) is required for HOTAIR-mediated TNBC growth and colony formation. YTHDC1 overexpression can compensate for HOTAIR mutation at this single m6A site. We demonstrate that chromatin association of HOTAIR is impaired by mutation of this single m6A site and can also be restored by overexpression of YTHDC1. Finally, using a reporter system, we show that YTHDC1 mediates repression by HOTAIR in the absence of PRC2. Overall, our results suggest a model where m6A modifications on HOTAIR enable interaction with YTHDC1 to retain HOTAIR on chromatin and enable repression of its target genes to alter TNBC cell properties.

Results

HOTAIR contains multiple sites of m6A modification in breast cancer cell lines

To investigate the possibility that m6A regulates the function of HOTAIR in a mechanism similar to its regulation of lncRNA Xist, we investigated previous studies in human cells where m6A sites have been mapped genome wide. We searched the CVm6A database[25] to identify any previously mapped sites of m6A modification in HOTAIR. HOTAIR contains 3 m6A peaks mapped in HeLa cells, although the enrichment score is low for these sites (Figure S1). To evaluate m6A methylation of HOTAIR in relevant breast cancer cells, we performed m6A RNA Immunoprecipitation (meRIP) qRT-PCR in MCF-7 cells. We initially chose to analyze MCF-7 cells as this cell line expresses detectable levels of endogenous HOTAIR – about 10-fold higher expression than the MDA-MB-231 TNBC cell line[24]. A significant portion of HOTAIR was recovered upon immunoprecipitation with the anti-m6A antibody (26.2%, p=0.006), similar to an m6A modified region of the positive control *EEF1A1* (Figure 1B).

To confirm m6A modification of HOTAIR in other breast cancer cell contexts, we generated a stable MDA-MB-231 cell line with transgenic overexpression of HOTAIR. The MDA-MB-231 is a TNBC cell line that expresses low levels of endogenous HOTAIR, less than 1 copy per cell[24] (see Figure 3A). The transgenic overexpression of HOTAIR is proposed to mimic the high levels of HOTAIR observed in patients with aggressive TNBC and results in increased cancer aggressiveness of MDA-MB-231 cells[12]. Similar to what was observed in MCF-7 cells, meRIP in MDA-MB-231 cells expressing transgenic HOTAIR resulted in significant HOTAIR recovery (27.1%, p=0.001). These results demonstrate that HOTAIR is m6A modified in multiple breast cancer contexts.

To identify single nucleotide sites of m6A modification, we performed a modified m6A eCLIP protocol[26] on polyA-selected RNA from MCF-7 and MDA-MB-231 breast cancer cells (Figure S2A). In MCF-7 cells, we identified one m6A site within the *HOTAIR* transcript at adenosine 783 (Figure 1D, Table S1). m6A sites were mapped in MDA-MB-231 cells with and without expression of transgenic HOTAIR (Table S1). m6A was consistently detected at adenosine 783 in both endogenous and transgenic HOTAIR. Ten additional m6A sites in HOTAIR were identified in the MDA-MB-231 cellular context (Figure 1D, Table S1).

We reasoned that if HOTAIR is consistently and specifically m6A modified, it would be through the canonical m6A methyltransferase METTL3/14 complex. To test this prediction, we performed shRNA mediated depletion of METTL3, METTL14, and the adaptor protein WTAP in MCF-7 cells (Figure S2B). Briefly, we designed 2 shRNAs for each target and performed stable lentiviral transductions of MCF-7 cells with the targeted shRNAs and a scramble control. We next performed meRIP in cell lines where we observed the most efficient knockdown. We observed a ~3 to 5-fold reduced recovery of HOTAIR relative to non-targeting controls ($p<0.01$) (Figure S2C). Together, these results demonstrate the role of the METTL3/14 complex in depositing m6A methylation on HOTAIR.

Nucleotide A783 is important for the ability of HOTAIR to promote breast cancer cell proliferation and colony formation

Nucleotide A783 was consistently methylated within HOTAIR in our m6A mapping experiments, in endogenous or overexpressed contexts. We examined the surrounding sequence of this site in HOTAIR for the canonical m6A 'DRACH' motif. Interestingly, this modification occurred in a non-canonical 'GAACG' within a loop of a stem-loop region of the HOTAIR secondary structure[27,28] (Figure S3A). To directly test the functional role of A783, we mutated the adenosine to uracil at position 783 ($HOTAIR^{A783U)}$. We then mapped m6A sites in MDA-MB-231 cells overexpressing the $HOTAIR^{A783U}$ mutant as above (Table S1). Both wild-type (WT) and the mutant form of HOTAIR were expressed at similar levels, with approximately 5,000 transcripts per cell (Figure 2A). These

levels resemble the high levels of HOTAIR observed in samples from cancer patients[29]. While m6A was no longer detected at adenosine 783 when this site was mutated to uracil, 5 out of 6 of the m6A sites were identified that were also consistently detected in transgenic WT HOTAIR, as well as 2 additional unique m6A sites (Table S1, Figure 1B). This suggests that there is no obvious dependency on the constitutive m6A783 for other methylation events, but that this site could alter the overall landscape of HOTAIR m6A modification.

To determine the effect of the A783U mutation on HOTAIR-mediated breast cancer cell growth, we measured the doubling time of MDA-MB-231 cells expressing WT and A783U mutant HOTAIR. As described above, we overexpressed HOTAIR and the $HOTAIR^{A783U}$ mutant in MDA-MB-231 cells, with overexpression of an antisense sequence luciferase mRNA (Anti-Luc) as a control. We observed a similar ~5,000-fold induction of WT and mutant HOTAIR (Figure 2A). We next performed cell proliferation assays by plating 5,000 cells in a 96-well dish and analyzing confluency every 2 hours over a period of 48 hours. We observed that MDA-MB-231 cells overexpressing WT HOTAIR had a shorter doubling time (~26 hours) than cells overexpressing Anti-Luc (~28.5 hours, $p<0.001$) (Figures S3B, 2B). Surprisingly, the single nucleotide mutation of A783U in HOTAIR abolished its ability to enhance MDA-MB-231 cell proliferation; cells expressing $HOTAIR^{A783U}$ had a longer doubling time than those expressing WT HOTAIR and grew similarly to cells containing the Anti-Luc control (~28.6 hours, $p=0.004$). To examine the role of A783 of HOTAIR in mediating colony formation, the same MDA-MB-231 cell lines were plated in a soft agar assay. While overexpression of WT HOTAIR induced a significant increase in percent colony area (~4-fold, $p=0.01$) and colony size (~3-fold, $p=0.04$), overexpression of A783U HOTAIR resulted in colonies that grew similarly to cells overexpressing the Anti-Luc control (Figure 2C-F). Altogether, these results suggest that m6A modification of adenosine 783 in HOTAIR is key for mediating aggressiveness of TNBC.

hnRNP B1 is not a direct m6A reader in MCF-7 cells

hnRNP A2/B1 has previously been suggested to be a reader of m6A, and the B1 isoform has a high affinity for binding HOTAIR[24,30,31]. However, comparing our previously generated eCLIP results for hnRNP B1[32] to the m6A eCLIP, both performed in MCF-7 cells, we found that, out of 10,470 m6A sites, only 417 (4%) were identified to contain an hnRNP B1 binding site within 1,000 nucleotides (Figure S4A). Upon mapping hnRNP B1 signal intensity relative to the nearby m6A site, we observed that hnRNP B1 is depleted directly over m6A sites (Figure S4B). These results suggest that hnRNP B1 is not a direct m6A reader, although m6A may indirectly promote its recruitment in some contexts (see Discussion). When comparing hnRNP B1 binding in HOTAIR with m6A sites, B1 binding peaks in MCF-7 cells occur in m6A-free regions of HOTAIR. Conversely, data from *in vitro* eCLIP analysis of B1 binding to unmodified HOTAIR reveal additional B1 binding peaks in Domain 1 of HOTAIR, one of which occurs near several m6A sites (Figure

S4C). Altogether, these data suggest that while m6A is not likely to directly recruit hnRNP B1 as a reader, it may contribute to hnRNP B1 binding, perhaps by modulating HOTAIR structure.

YTHDC1 regulates the ability of HOTAIR to induce breast cancer proliferation and colony formation

YTHDC1 is a nuclear-localized m6A reader that binds m6A sites in noncoding RNAs, including the Xist lncRNA and LINE-1 elements[6,9]. We reasoned that YTHDC1 was a strong candidate for interaction with HOTAIR, which is a lncRNA that is also primarily nuclear-localized. To determine if YTHDC1 interacts with HOTAIR, we performed RNA immunoprecipitation (RIP) qRT-PCR using an antibody to YTHDC1. In both MDA-MB-231 cells overexpressing transgenic HOTAIR, and MCF-7 cells expressing endogenous HOTAIR, a significant portion of HOTAIR RNA was recovered when using antibodies specific against YTHDC1 (17.4%, p=0.04; 2.6%, p=0.003, respectively) (Figure 3A, B).

To test the role of YTHDC1 in HOTAIR's ability to enhance breast cancer cell proliferation, we overexpressed or stably knocked down YTHDC1 in the context of WT or A783U HOTAIR overexpression in MDA-MB-231 cells (Figure 3C-D). We noted that YTHDC1 protein levels tended to be ~2.3 fold higher in cells containing WT HOTAIR compared to A783U mutant HOTAIR (Figure 3D). Although this difference was not significant (p=0.16), it suggests a potential positive relationship between WT HOTAIR RNA and YTHDC1 protein levels.

Next, we used the MDA-MB-231 cell lines we generated to analyze proliferation as described above. Growth of MDA-MB-231 cells overexpressing WT HOTAIR was not significantly altered by YTHDC1 dosage (0.96 fold change p=0.16, 1.08 fold change p=0.26 for pLX-DC1 and shDC1, respectively), yet there was a trend towards decreased doubling time with increasing YTHDC1. In contrast, cells with A783U mutant HOTAIR had significant differences in doubling time with overexpression or knockdown of YTHDC1 (Figure 3E). Overexpression of YTHDC1 led to significantly faster growth of MDA-MB-231 cells containing A783U mutant HOTAIR (0.84-fold change in doubling time, p=0.003), with proliferation rates comparable to cells expressing WT HOTAIR. Knockdown of YTHDC1 in cells containing $HOTAIR^{A783U}$ was particularly potent in reducing the growth rate (~1.2-fold increase in doubling time, p=0.008) demonstrating a role for YTHDC1 in mediating HOTAIR's ability to enhance proliferation of breast cancer cells through A783.

To determine the ability of MDA-MB-231 cells with YTHDC1 overexpression and knockdown to grow under anchorage-independent conditions, we performed soft agar colony formation assays. Cells containing overexpression of YTHDC1 had a significant increase in percent colony area (~16.5-fold increase, p=0.006 for WT HOTAIR, ~10.7-fold increase p=0.01 for $HOTAIR^{A783U}$) (Figure

3F). When YTHDC1 was overexpressed in cells containing WT HOTAIR, colony size (~4-fold, p=0.05) and count (~10-fold, p=0.03) were significantly elevated (Figure 3G-H). In cells containing A783U mutant HOTAIR, YTHDC1 overexpression mediated a significant increase in colony count (~15-fold, p=0.02) but not colony size (~1.7-fold, p=0.07) (Figure 3G-H). The strong effect of YTHDC1 overexpression on colony formation in both WT and A783U mutant HOTAIR suggests that YTHDC1 mediates anchorage-independent growth in HOTAIR-expressing MDA-MB-231 cells. These effects were not consistent in MCF-7 cells, where YTHDC1 levels did not affect colony formation (Figure S5), perhaps suggesting a specific effect in TNBC cells.

High *HOTAIR* levels are associated with aggressiveness in breast cancer patients with high *YTHDC1* expression

To further explore a clinical role for HOTAIR and YTHDC1 in breast cancer, we used GEPIA2[33] to analyze the relationship of *HOTAIR* and *YTHDC1* expression in publicly available outcomes data from breast cancer patient primary tumors. Across all breast cancer patient samples, *YTHDC1* is generally expressed, ranging roughly five-fold at the mRNA level. HOTAIR levels vary more widely, with some samples not expressing the lncRNA. Because of these different expression profiles, there is only a very modest positive correlation between *HOTAIR* and *YTHDC1* (R=0.092, p=0.0025) (Figure S6A). To further investigate *HOTAIR* and *YTHDC*1 in breast tumors, we used the Kaplan-Meier Plotter to analyze recurrence-free and overall survival of breast cancer patients[34] as well as UALCAN (a tool for analyzing cancer OMICS data) to determine gene expression in normal breast tissue versus breast tumor specimens[35]. Consistent with previous studies, high expression of *HOTAIR* is indicative of a shorter time to recurrence (HR=1.41, p=6.3e-05) (Figure 4A) and shorter overall survival (HR=1.65, p=0.0084) (Figure S6B). *HOTAIR* RNA expression is increased in breast cancer specimens ~7-fold compared to normal breast tissues (p=1.62e-12), with the highest *HOTAIR* expression (~14.5-fold increase) observed in Stage 4 disease (p=5.36e-04) (Figure S6C-D). The reverse is true for *YTHDC1*, with high levels corresponding to longer disease-free status (HR=0.69, p=2.5e-11) (Figure 4B) and overall survival (HR=0.73, p=0.0088) (Figure S7A) and a modest decrease (~10%) in mRNA levels in tumor compared to normal tissue (p=1.14e-06) (Figures 4C, S7B). Interestingly, YTHDC1 protein is higher in tumor samples compared to normal tissue (p=6.7e-09) (Figure 4D, S7C). This could be because in general there are fewer epithelial cells in normal breast compared to the number of carcinoma cells in breast tumors[36], and may suggest a significant amount of translational regulation for the YTHDC1 mRNA.

To examine *YTHDC1* in relation to *HOTAIR* in breast cancer outcomes, we assessed recurrence-free and overall survival based on *HOTAIR* expression in cohorts of tumors expressing either high or low levels of *YTHDC1* mRNA. In the context of high *YTHDC1* expression, *HOTAIR* is even more strongly indicative of risk for shorter time to recurrence (HR=1.93, p=3.2e-05) (Figure 4E) and overall

survival (HR=2.1, p=0.0012) (Figure S7D) compared to *HOTAIR* alone (Figures 4B, S6B). On the background of low *YTHDC1*, *HOTAIR* has a less impressive effect on disease-free survival (HR=1.33, p=0.007) (Figure 4F), more similar to the effect of *HOTAIR* alone (Figure 4B), and on overall survival, where *HOTAIR* expression is no longer a significant prognostic indicator (p=0.23) (Figure S7E). Altogether, these patient outcomes data are consistent with high *YTHDC1* levels supporting the ability of HOTAIR to affect breast cancer aggressiveness.

Mutation at A783 of HOTAIR results in decreased interaction with YTHDC1 *in vitro*, but does not abolish HOTAIR methylation or YTHDC1 interaction at other sites *in vivo*

To determine if nucleotide A783 in HOTAIR recruits YTHDC1 via m6A modification, we generated PP7-tagged *in vitro* transcribed RNA of domain 2 of WT or A783U HOTAIR and performed *in vitro* m6A methylation with purified METTL3/14[37] and S-adenosylmethionine as a methyl donor. We then transfected HEK293 cells with an expression plasmid containing FLAG-tagged YTHDC1 and obtained protein lysates. The *in vitro HOTAIR* transcripts were tethered to IgG-coupled magnetic beads via a PP7-Protein A fusion protein and incubated with FLAG-YTHDC1-containing protein lysates. Beads were washed and the relative recovery of FLAG-YTHDC1 was determined by anti-FLAG Western Blot (Figure 5A). WT HOTAIR interaction with YTHDC1 was enhanced when the transcript was m6A-modified (~3-fold increase, p=0.04), while A783U HOTAIR interaction with YTHDC1 was not significantly altered by the addition of m6A (~1.3-fold change, p=0.6) (Figure 5B-C).

To characterize changes to the molecular interactions that occur with mutation of A783 in breast cancer cells, we performed m6A and YTHDC1 RIP experiments on MDA-MB-231 cells overexpressing WT or A783U HOTAIR (Figure S8A-B). Surprisingly, we did not see any significant changes in HOTAIR recovery in either experiment (~1.2-fold change, p=0.5; 1.1-fold change, p=0.8 for m6A and YTHDC1 RIP, respectively). The A783U HOTAIR maintains m6A modifications at other sites within the RNA, which we have mapped in the overexpression context (Table S1). These sites are likely sufficient for HOTAIR recovery when immunoprecipitating YTHDC1. However, modification of A783, in particular, appears to be important in mediating the physiological effects observed by HOTAIR overexpression, likely by YTHDC1 binding to A783 in a methylation-dependent manner, as observed in the *in vitro* experiment (Figure 5B-C).

m6A and YTHDC1 mediate chromatin retention and expression of HOTAIR

Based on the differences observed between cell lines containing WT and A783U HOTAIR and the function of HOTAIR in chromatin-mediated gene repression, we investigated whether chromatin association of HOTAIR was altered in these cells. We performed fractionation of MDA-MB-231 cells containing WT or A783U HOTAIR or an antisense-Luciferase control into cytoplasm, nucleoplasm, and chromatin fractions (Figure 5D, see Methods) We isolated RNA from each fraction and performed qRT-PCR for HOTAIR and GAPDH. Cells overexpressing WT HOTAIR had significantly more chromatin-associated HOTAIR (~4.3-fold) than cells expressing A783U HOTAIR (p=0.05) (Figure 5E), though overall levels of HOTAIR are unchanged (Figure 2A).

To examine the effect of YTHDC1 levels on HOTAIR chromatin association, we performed a similar fractionation experiment in MDA-MB-231 cells expressing WT or A783U HOTAIR with overexpression or knockdown of YTHDC1 (Figure S8C). While YTHDC1 levels did not significantly alter WT HOTAIR chromatin association, overexpression of YTHDC1 increased A783U HOTAIR chromatin association ~1.9-fold to similar levels as WT HOTAIR (p=0.05), and knockdown resulted in a significant ~10-fold decrease in chromatin association (p=0.01) (Figure 5F).

While HOTAIR expression levels remained similar for pLX-DC1 overexpression lines compared to shNT control lines (0.8 fold change, p=0.3), they were significantly decreased by ~5 to 10-fold in YTHDC1 knockdown lines for both WT and A783U mutant *HOTAIR* relative to shNT cell lines (p=3.24e-10) (Figure 5G). These results suggest that YTHDC1 regulates the expression or stability of HOTAIR, independently of A783. To investigate the role of other m6A sites within HOTAIR, we generated HOTAIR overexpression constructs containing 6 or 14 adenosine-to-uracil mutations (6xAU and 14xAU, respectively). While WT and A783U HOTAIR expression levels were similarly high, there was a ~50-fold decrease in expression of 6xAU or 14xAU HOTAIR (Figure 5H). This suggests that other m6A sites within HOTAIR mediate its high expression levels in breast cancer cells.

YTHDC1 contributes to gene repression by HOTAIR in the absence of PRC2, independent of its role in chromatin recruitment or RNA expression level

To determine the effect of YTHDC1 on transcriptional repression mediated by HOTAIR, we used previously generated reporter cell lines that contain HOTAIR artificially directly tethered to chromatin upstream of a luciferase reporter gene to repress expression, independent of PRC2[16] (Figure 6A). We confirmed that HOTAIR tethered upstream of the luciferase reporter reduced luciferase expression using both qRT-PCR (~2.3-fold lower, p=8.0e-12) and luciferase assay (~3.1-fold lower, p=0.002) (Figure 6B, C). We also performed m6A eCLIP to confirm that *HOTAIR* was m6A modified in this context and detected 10 m6A sites within *HOTAIR*, including

A783 (Table S1). To test the role of YTHDC1 in the repression mediated by HOTAIR, we used 3 different siRNAs to knock down YTHDC1 relative to a non-targeting control (~2-fold decrease in protein levels, p=0.02) in the HOTAIR-tethered cells lacking the essential PRC2 subunit EED (Figure 6D). Knockdown of YTHDC1 resulted in significantly higher luciferase RNA levels in these cells (p=3.1e-05) (Figure 6E). Luciferase enzymatic activity also increased upon YTHDC1 knockdown (p=0.003) (Figure 6F). YTHDC1 knockdown did not affect *HOTAIR* RNA levels in this context (~1.2-fold increase, p=0.8) (Figure S9A-B), indicating that the effects observed on luciferase expression were likely due to disruption of the HOTAIR gene repression mechanism via depletion of YTHDC1 protein rather than loss of HOTAIR expression.

Discussion

Like m6A on mRNAs, it is becoming evident that m6A on lncRNAs is both functionally diverse and context dependent. Here, we demonstrate that m6A and the m6A reader YTHDC1 function to enable transcriptional repression by HOTAIR which is analogous to the repressive function demonstrated for the lncRNA Xist[6,8]. Our results reveal a mechanism whereby m6A modification of HOTAIR at a specific adenosine residue mediates interaction with YTHDC1, in turn enabling transcriptional interference by HOTAIR which enhances TNBC properties including proliferation and colony formation.

Function of specific m6A sites in HOTAIR

While several m6A sites were identified within HOTAIR when overexpressed, we only detected one m6A site in the endogenously expressed context in MCF-7 cells, making it the most consistently present methylation site. MDA-MB-231 cells overexpressing HOTAIR containing a mutation of this single m6A-modified adenosine had a defect in HOTAIR-mediated proliferation and colony formation, although A783U mutant HOTAIR maintained m6A modification at other sites and interaction with YTHDC1 at those sites *in vivo*. It is possible that the A783 m6A site specifically is a high-affinity site for YTHDC1 interaction based on our *in vitro* analysis where YTHDC1 association with methylated domain 2 of HOTAIR was dependent on this site. In line with this hypothesis, we observe a decrease in chromatin-association when A783 of HOTAIR is mutated, which is recovered upon overexpression of YTHDC1. While it is clear that m6A modification of A783 in HOTAIR is important for mediating its effects in breast cancer, other m6A sites within HOTAIR appear to play a role in enabling its high expression levels, potentially through transcript stabilization. When we bypass the normal mechanism of chromatin association using a direct tethering approach for HOTAIR (Figure 6A)[16], YTHDC1 is no longer required for chromatin association or high expression level, and yet YTHDC1 is required for gene repression, suggesting a direct role in shutting

down transcription. Our work emphasizes the importance of studying the function of individual m6A sites, as each m6A site has the potential to contribute to the function of an RNA in different ways.

m6A in gene repression and heterochromatin formation

HOTAIR and other lncRNAs make many dynamic and multivalent interactions with proteins that interact with other proteins, RNA molecules, and chromatin. In the nucleus, YTHDC1 is a key interactor with m6A-modified RNA. This study and previous work demonstrate that YTHDC1 acts to regulate transcriptional repression by lncRNAs[6], although the mechanism by which this is accomplished remains ambiguous. Our data suggest that YTHDC1-mediated transcriptional repression occurs upstream of chromatin modification by PRC2. This supports the mechanism of transcriptional interference by HOTAIR proposed by Portoso et. al.[16] (Figure 1A) and suggests that YTHDC1 is an important factor that mediates repression by HOTAIR. While a similar mechanism may mediate repression by Xist, it is still unclear how YTHDC1 binding to a repressive lncRNA mediates transcriptional interference and repression. Analysis of the YTHDC1 interaction network has identified interactions with components of the PRC2 complex[38], but our work demonstrates that PRC2 is not required for YTHDC1-dependent repression of gene expression by HOTAIR. Thus, further experiments are needed to determine the mechanisms used by YTHDC1 to enable transcriptional silencing.

There is an elegant and complex interplay between chromatin, m6A, splicing, and transcription[39–42]. HOTAIR-interacting RNA binding proteins hnRNP B1 and YTHDC1, which mediate HOTAIR-induced repression, are regulated by m6A and have roles in splicing[31,43–46]. In the case of YTHDC1, previous studies have demonstrated its localization in defined nuclear puncta that interact with nuclear speckles and splicing machinery[44,47]. Interestingly, recent work has demonstrated the potential for other cytoplasmic YTH proteins to facilitate phase separation of m6A-modified RNA molecules[48], a process which may also contribute to heterochromatin domain formation[49]. Future work will be necessary to examine the potential contribution of YTHDC1-mediated phase separation to transcriptional repression and heterochromatin formation by lncRNAs.

Divergence in m6A function for different classes of RNAs

The role of YTHDC1 in mediating chromatin association of and repression by HOTAIR is interesting in the context of the recently identified broad nuclear role of YTHDC1 in regulation of transcription and chromatin state in mouse embryonic stem cells[9]. While in this case it was demonstrated that YTHDC1 mediates degradation of m6A-modified chromatin-associated regulatory RNAs, our work raises the question and possibility that YTHDC1 might also mediate transcriptional repression and/or heterochromatin directly through interaction with regulatory RNAs. Our work also shows that, rather than degradation of HOTAIR, m6A sites in HOTAIR mediate its high

expression in breast cancer via YTHDC1. An important distinction between HOTAIR and the chromatin-associated regulatory RNAs investigated by Liu *et. al*[9] is that HOTAIR regulates genes in *trans* versus *cis*. Liu *et. al* found that YTHDC1 mediates degradation of *cis*-regulatory RNAs by the NEXT complex to slow downstream transcription of their target genes; however, in the case of HOTAIR, YTHDC1 mediates chromatin retention of a *trans*-regulatory lncRNA, presumably helping it to repress its target genes in *trans*. We hypothesize that chromatin retention of HOTAIR stabilizes it because stable retention of HOTAIR on chromatin as heterochromatin forms is likely to make it inaccessible to factors that mediate its degradation. Our experiments where HOTAIR is tethered to chromatin in a reporter cell line illustrates this, as knockdown of YTHDC1 did not alter the level of HOTAIR in the context where it is constitutively tethered to chromatin (Figure S9C). It is likely that YTHDC1 performs multiple functions within the nucleus, and that its effects on its target RNAs are context dependent, such as on other nearby RNA binding proteins and local chromatin state.

Our work also highlights the fate of HOTAIR-YTHDC1 interaction which is distinctly different from mRNAs whose nuclear export is mediated by YTHDC1[50]. In contrast, we show that YTHDC1 mediates chromatin retention of the primarily nuclear-localized HOTAIR lncRNA. Also, while one specific m6A site at A783 is important for mediating chromatin retention and the physiological effects of HOTAIR in breast cancer, other m6A sites play a role in overall expression or stability (Figure 7). It is likely that the RNA context and other proteins that either interact directly with YTHDC1 or the RNA molecules it binds to dictate the effects of YTHDC1 binding to its targets. Additional studies on how YTHDC1 interacts with specific RNA targets, chromatin, and other proteins in the nucleus will shed light on the mechanisms of YTHDC1 in chromatin regulation.

Potential for broad m6A roles for lncRNAs in cancer

Many lncRNAs have been shown to mediate repression of genes in *trans*, especially in the context of cancer. In addition to HOTAIR, these include TUG1 and MEG3, both of which have been shown to interact with PRC2 and induce H3K27me3 of their targets. It has been demonstrated that TUG1 contains multiple m6A sites[51] and that MEG3 can induce m6A modification of its target PTEN[52]. Whether these and other repressive lncRNAs employ m6A or YTHDC1 to accomplish repression of their targets and how m6A levels regulate cancer progression in specific settings are open questions.

Conclusion

The context dependency of m6A function is a theme in m6A biology. With various roles in pluripotency and development and in disease states such as cancer, m6A on different RNA molecules regulates their fate and functional output in different ways. Our work illustrates the context of three specific m6A functions: enabling chromatin retention, promoting high levels of lncRNA expression,

and transcriptional repression. We further highlight the importance of one specific m6A site within a lncRNA that contains multiple sites of modification. Further research into the mechanism and frequency of m6A modification at single nucleotide sites as well as how m6A at these sites mediates affinity for different RNA binding proteins will shed light on the ultimate function of specific m6A sites within individual RNA molecules.

As the only primarily nuclear m6A reader, YTHDC1 has the potential to interact with m6A-containing RNA molecules at the site of transcription on chromatin. The outcome of this interaction appears to be dictated by the identity of the RNA molecule, including whether it functions in *cis* or *trans*, but ultimately has the potential to result in chromatin regulation. Our work demonstrates the importance of YTHDC1 in mediating HOTAIR chromatin retention and transcriptional repression independent of PRC2, revealing a new layer of regulation by m6A at a specific residue within HOTAIR. Overall, this provides insight into mechanisms of how m6A regulates lncRNA-mediated transcriptional repression.

Materials and Methods

Cell Culture

MCF-7 cells were maintained in RPMI media (11875093, Invitrogen) and MDA-MB-231 and 293T cells were maintained in DMEM media (MT10013CV, Fisher Scientific). Media contained 10% FBS (F2442-500ML, Sigma-Aldrich) and Pen-Strep (MT30002CI, Fisher Scientific) and cells were grown under standard tissue culture conditions. Cells were split using Trypsin (MT25053CI, Fisher Scientific) according to manufacturer's instructions.

MDA-MB-231 cells overexpressing WT HOTAIR, A783U mutant HOTAIR, or Anti-Luciferase were generated as previously described using retroviral transduction[24]. Stable knockdown of METTL3, METTL14, WTAP, and YTHDC1 and overexpression of YTHDC1 was performed by lentivirus infection of MCF-7 cells or MDA-MB-231 cells overexpressing HOTAIR or A783U mutant HOTAIR via Fugene HD R.8 with pLKO.1-blasticidin shRNA constructs or a pLX304 overexpression construct as noted in Table S2. Cells were selected with 5 µg/mL blasticidin (Life Technologies). The nontargeting shRNA pLKO.1-blast-SCRAMBLE was obtained from Addgene (Catalog #26701).

Plasmid Construction

The pBABE-puro retroviral vector was used for overexpression of lncRNAs. The spliced HOTAIR transcript (NR_003716.3) was synthesized and cloned into the pBABE-puro retroviral vector by GenScript. An antisense transcript of the firefly luciferase gene (AntiLuc) was amplified from the pTRE3G-Luciferase plasmid (Clonetech), then cloned into the pBABE-puro retroviral vector. These were generated in a previous publication[24].

To create the A783U mutant HOTAIR overexpression plasmid, staggered QuikChange oligos AG66/AG67 were used to generate the A783U mutation in pTRE3G-HOTAIR using the QuikChange Site Directed Mutagenesis Kit (Agilent 200519) to generate pTRE3G-A783U_HOTAIR. A 1.6Kb fragment of A783U mutant HOTAIR was amplified with primers AG68/AG69 from pTRE3G-A783U_HOTAIR for cloning into pBABE-Puro-HOTAIR cut with XcmI and BamHI by Gibson Assembly. Oligonucleotide sequences are noted in Table S3. All constructs were confirmed by sequencing. pBABE-Puro-6xAU_HOTAIR and pBabe-Puro-14xAU_HOTAIR were synthesized and cloned by GenScript.

Plasmids for the knockdown of METTL3, METTL14, WTAP, and YTHDC1 were generated by cloning the shRNA (RNAi Consortium shRNA Library) from pLKO.1-puro into the pLKO.1-blast backbone (Addgene #26655). All plasmids were confirmed by sequencing.

m6A enhanced crosslinking immunoprecipitation:

polyA isolation and RNA fragmentation

For each experiment, approximately 100 µg of total RNA was isolated from cells with Trizol according to manufacturer's instructions. 10 µg PolyA RNA was isolated using Magnosphere® Ultrapure mRNA Purification Kit (Takara) according to manufacturer's instructions. PolyA RNA was ethanol precipitated with 2.5 M Ammonium Acetate and 70% ethanol in a solution containing 50 µg/ml GlycoBlue Coprecipitant (AM9515, Invitrogen). RNA was resuspended in 10 µl and fragmented with 10x Fragmentation Buffer (AM8740, Invitrogen) at 75°C for 8 minutes and immediately quenched with 10x Stop Reagent (AM8740, Invitrogen) and placed on ice to generate fragments 30-150 nucleotides in length.

Anti-m6A-RNA crosslinking and bead conjugation

Crosslinked RNA-Antibody was generated as previously described[53]. Fragmented RNA was resuspended in 500 µl Binding/Low Salt Buffer (50 mM Tris-HCl pH 7.4, 150 mM Sodium Chloride, 0.5% NP-40) containing 2 µl RNase Inhibitor (M0314, NEB) and 10 µl m6A antibody (ab151230, Abcam), and incubated for 2 hours at room temperature with rotation. RNA-Antibody sample was transferred to one well of a 12-well dish and placed in a shallow dish of ice. Sample was crosslinked twice at 150 mJ/cm^2 using a

Stratagene Stratalinker UV Crosslinker 1800 and transferred to a new tube. 50 µl Protein A/G Magnetic Beads (88803, Pierce) were washed twice with Binding/Low Salt Buffer, resuspended in 100 µl Binding/Low Salt Buffer, and added to crosslinked RNA-Antibody sample. Beads were incubated at 4°C overnight with rotation.

eCLIP library prepration

RNA was isolated and sequencing libraries were prepared using a modified enhanced CLIP protocol[54]. Beads were washed twice with High Salt Wash Buffer (50 mM Tris-HCl pH 7.4, 1 M Sodium Chloride, 1 mM EDTA, 1% NP-40, 0.5% Sodium Deoxycholate, 0.1% Sodium Dodecyl Sulfate), once with Wash Buffer (20 mM Tris-HCl pH 7.4, 10 mM Magnesium Chloride, 0.2% Tween-20), once with Wash Buffer and 1x Fast AP Buffer (10 mM Tris pH 7.5, 5 mM Magnesium Chloride, 100 mM Potassium Chloride, 0.02% Triton X-100) combined in equal volumes, and once with 1x Fast AP Buffer. Beads were resuspended in Fast AP Master Mix (1x Fast AP Buffer containing 80U RNase Inhibitor (M0314, NEB), 2U TURBO DNase (AM2238, Invitrogen), and 8U Fast AP Enzyme (EF0654, Thermo Scientific)) was added. Samples were incubated at 37°C for 15 minutes shaking at 1200 rpm. PNK Master Mix (1x PNK Buffer (70 mM Tris-HCl pH 6.5, 10 mM Magnesium Chloride), 1 mM Dithiothreitol, 200U RNase Inhibitor, 2U TURBO DNase, 70U T4 PNK (EK0031, Thermo Scientific)) was added to the samples and they incubated at 37°C for 20 minutes shaking at 1200 rpm.

Beads were washed once with Wash Buffer, twice with Wash Buffer and High Salt Wash Buffer mixed in equal volumes, once with Wash Buffer, once with Wash Buffer and 1x Ligase Buffer (50 mM Tris pH 7.5, 10 mM Magnesium Chloride) mixed in equal volumes, and twice with 1x Ligase Buffer. Beads were resuspended in Ligase Master Mix (1x Ligase Buffer, 1 mM ATP, 3.2% DMSO, 18% PEG 8000, 16U RNase Inhibitor, 75U T4 RNA Ligase I (M0437, NEB)), two barcoded adaptors were added (X1a and X1b, see Table S4), and samples were incubated at room temperature for 75 minutes with flicking every 10 minutes. Beads were washed once with Wash Buffer, once with equal volumes of Wash Buffer and High Salt Wash Buffer, once with High Salt Wash Buffer, once with equal volumes of High Salt Wash Buffer and Wash Buffer, and once with Wash Buffer. Beads were resuspended in Wash Buffer containing 1x NuPAGE LDS Sample Buffer (NP0007, Invitrogen) and 0.1M DTT, and incubated at 70°C for 10 minutes shaking at 1200 rpm.

Samples were cooled to room temperature and supernatant was ran on Novex NuPAGE 4-12% Bis-Tris Gel (NP0321, Invitrogen). Samples were transferred to nitrocellulose membrane, and membranes were cut and sliced into small pieces between 20 kDa and 175 kDa to isolate RNA-antibody complexes. Membrane slices were incubated in 20% Proteinase K (03508838103, Roche) in PK Buffer (100 mM Tris-HCl pH 7.4, 50 mM NaCl, 10 mM EDTA) at 37°C for 20 minutes shaking at 1200 rpm. PK Buffer containing 7M urea was added to samples and samples were incubated at 37°C for 20 minutes shaking at 1200 rpm. Phenol:Chloroform:Isoamyl

Alcohol (25:24:1) (P2069, Sigma-Aldrich) was added to samples and samples were incubated at 37°C for 5 minutes shaking at 1100 rpm. Samples were centrifuged 3 minutes at 16,000 x *g* and aqueous layer was transferred to a new tube.

RNA was isolated using RNA Clean & Concentrator-5 Kit (R1016, Zymo) according to manufacturer's instructions. Reverse transcription was performed using AR17 primer (Table S4) and SuperScript IV Reverse Transcriptase (18090010, Invitrogen). cDNA was treated with ExoSAP-IT Reagent (78201, Applied Biosystems) at 37°C for 15 minutes, followed by incubation with 20 mM EDTA and 0.1M Sodium Hydroxide at 70°C for 12 minutes. Reaction was quenched with 0.1M Hydrochloric Acid. cDNA was isolated using Dynabeads MyONE Silane (37002D, ThermoFisher Scientific) according to manufacturer's instructions. 20% DMSO and rand3Tr3 adaptor (Table S4) was added to samples, and samples were incubated at 75° for 2 minutes. Samples were placed on ice and Ligation Master Mix (1x NEB Ligase Buffer, 1mM ATP, 25% PEG 8000, 15U T4 RNA Ligase I (NEB)) was added to samples. Samples were mixed at 1200 rpm for 30 seconds prior to incubation at room temperature overnight.

cDNA was isolated using Dynabeads MyONE Silane according to manufacturer's instructions and eluted with 10 mM Tris-HCl pH 7.5. A 1:10 dilution of cDNA was used to quantify the cDNA library by qPCR using a set of Illumina's HT Seq primers, and Ct values were used to determine number of cycles for PCR amplification of cDNA. The undiluted cDNA library was amplified by combining 12.5μL of the sample with 25μL Q5 Hot Start PCR Master Mix and 2.5μL (20μM) of the same indexed primers used previously. Amplification for the full undiluted sample used 3 cycles less than the cycle selected from the diluted sample. The PCR reaction was isolated using HighPrep PCR Clean-up System (AC-60050, MAGBIO) according to manufacturer's instructions.

The final sequencing library was gel purified by diluting the sample with 1x Orange G DNA loading buffer and running on a 3% quick dissolve agarose gel containing SYBR Safe Dye (1:10,000). Following gel electrophoresis, a long wave UV lamp was used to extract DNA fragments from the gel ranging from 175 to 300 base pairs. The DNA was isolated using QiaQuick MinElute Gel Extraction Kit (28604, Qiagen). The purified sequencing library was analyzed via TapeStation using DNA ScreenTape (either D1000 or HS D1000) according to the manufacturer's instructions to assess for appropriate size and concentration (the final library should be between 175 and 300 base pairs with an ideal concentration of at least 10nM).

Sequencing and analysis

Samples were sequenced at the Genomics and Microarray Shared Resource facility at University of Colorado Denver Cancer Center on an Illumina MiSeq or NovaSEQ6000 with 2x 150 base pair paired-end reads to generate 40 million raw reads for each sample. Computational analysis methods are described in [26]. Briefly, a custom Snakemake workflow was generated based on

the original eCLIP analysis strategies[54] to map reads to the human genome. To identify m6A sites, we used a custom analysis pipeline to identify variations from the reference genome at single-nucleotide resolution across the entire genome. We then employed an internally developed Java package to identify C-to-T mutations occurring 1) within the m^6A consensus motif 'RAC': 'R' is any purine, A or G; A being the methylated adenosine; and C where the mutation occurs; and 2) within a frequency range of greater than or equal to 2.5% and less than or equal to 50% of the total reads at a given position (with a minimum of 3 C-to-T mutations at a single site). The resulting m^6A sites were then compared to those identified in the corresponding input sample and any sites occurring in both were removed from the final list of m^6A sites (this eliminates any mutations that are not directly induced from the anti-m^6A antibody crosslinking).

m6A RNA Immunoprecipitation (meRIP)

Total RNA was isolated with TRIzol (15596018, Invitrogen) according to the manufacturer's instructions. RNA was diluted to 1 µg/µl and fragmented with 1x Fragmentation Buffer (AM8740, Invitrogen) at 75°C for 5 minutes. 1x Stop Reagent (AM8740, Invitrogen) was added immediately following fragmentation and samples placed on ice. 500 ng of input sample was reserved in 10 µl nuclease free water for qRT-PCR normalization. Protein A/G Magnetic Beads (88803, Pierce) were washed twice with IP Buffer (20 mM Tris pH 7.5, 140 mM NaCl, 1% NP-40, 2mM EDTA) and coupled with anti-m6A antibody (ab151230, Abcam) or an IgG control (NB810-56910, Novus) for 1 hour at room temperature. Beads were washed 3 times with IP Buffer. 10 µg fragmented RNA and 400U RNase inhibitor was added to 1 ml IP Buffer. Antibody-coupled beads were resuspended in 500 µl RNA mixture and incubated 2 hours to overnight at 4°C on a rotor. Beads were washed 5 times with cold IP Buffer. Elution Buffer (1x IP Buffer containing 10 U/µl RNase inhibitor and 0.5 mg/ml N6-methyladenosine 5'-monophosphate (M2780, Sigma-Aldrich) was prepared fresh and kept on ice. Samples were eluted with 200 µl Elution Buffer for 2 hours at 4°C on a rotor. Supernatant was removed and ethanol precipitated with 2.5M Ammonium Acetate, 70% Ethanol, and 50 µg/ml GlycoBlue Coprecipitant (Invitrogen AM9515). RNA was washed with 70% ethanol, dried for 10 minutes at room temperature, and resuspended in 10 µl nuclease free water. RNA was quantified by nanodrop and 200 ng RNA was reverse transcribed using High Capacity cDNA Reverse Transcription Kit (4368814, ThermoFisher Scientific) and quantified by qPCR, and fraction recovered was calculated from Input and IP values.

RNA Immunoprecipitation of YTHDC1

Actively growing cells from 70-90% confluent 15-cm dishes were trypsinized and washed twice with ice-cold 1x PBS. Cell pellet was resuspended in 1% V/V Formaldehyde (28908, Pierce) in 1x PBS and incubated at room temperature for 10 minutes on a rotor. Crosslinking was quenched with 0.25 M glycine at room temperature for 5 minutes. Cells were washed 3 times with ice-cold 1x PBS

and placed on ice. 20 µl Protein A/G beads were washed twice with RIPA Binding Buffer (50 mM Tris-HCl pH 7.4, 100 mM Sodium Chloride, 1% NP-40, 0.1% Sodium Dodecyl Sulfate, 0.5% Sodium Deoxycholate, 4 mM Dithiothreitol, 1x Protease Inhibitors), resuspended in 1 ml RIPA Binding Buffer, and split to two 0.5 ml aliquots. 2 µg YTHDC1 antibody (ab122340, Abcam) or an IgG Control (sc-2027, Santa Cruz Biotechnology) was added to beads and incubated for 2 hours at 4°C on a rotor. Fixed cells were resuspended in 1 ml RIPA Binding Buffer and placed in the Bioruptor Pico (B01060010, Diagenode) for 10 cycles of 30 seconds on, 30 seconds off. Lysates were digested with TURBO DNase for 5 minutes at 37°C with mixing at 1000 rpm and transferred to ice for 5 minutes. Lysates were clarified by centrifugation at 17,000*g* at 4°C for 10 minutes and supernatant was transferred to a new tube. 200U RNase Inhibitor was added to the 1 ml clarified lysate. A 5% aliquot was removed and processed downstream with IP samples. A 2% aliquot was removed and diluted with 1x SDS Sample Buffer (62.5 mM Tris-HCl pH 6.8, 2.5% SDS, 0.002% Bromophenol Blue, 5% β-mercaptoethanol, 10% glycerol) and protein input and recovery was monitored by Western Blot. Antibody-coupled beads were washed 3 times with RIPA Binding Buffer and resuspended in half of the remaining lysate. Samples were incubated overnight at 4°C on a rotor. Beads were washed 5 times with RIPA Wash Buffer (50 mM Tris-HCl pH 7.4, 1 M Sodium Chloride, 1% NP-40, 0.1% Sodium Dodecyl Sulfate, 0.5% Sodium Deoxycholate, 1 M Urea, 1x Protease Inhibitors) and resuspended in 100 µl RNA Elution Buffer (50 mM Tris-HCl pH 7.4, 5 mM EDTA, 10 mM Dithiothreitol, 1% Sodium Dodecyl Sulfate). Input sample was diluted with 1x RNA Elution Buffer. Formaldehyde crosslinks in both input and IP samples were reversed by incubation at 70°C for 30 minutes at 1000 rpm. Supernatant was transferred to a new tube and RNA was isolated using TRIzol-LS according to the manufacturer's instructions. Reverse transcription was performed on 100 ng RNA using SuperScript IV Reverse Transcriptase. qPCR was performed as described below.

RNA Isolation and qRT-PCR

RNA was isolated with TRIzol (Life Technologies) with extraction in chloroform followed by purification with the RNeasy kit (Qiagen). Samples were DNase treated using TURBO DNase (Ambion). Reverse transcription was performed using the cDNA High Capacity Kit (Life Technologies). qPCR was performed using Sybr Green master mix (Takyon, AnaSpec Inc.) using the primers listed in Table S5 on a C1000 Touch Thermocycler (BioRad). EEF1A1 primer sequences were obtained from the Magna MeRIP m6A kit (17-10499, Sigma-Aldrich). Sequences for Luciferase primers (LucR2) were obtained from a previous publication[55]. Three qPCR replicates were performed for each sample, and these technical replicates were averaged prior to analysis of biological replicates.

Cell Proliferation Assays

2,000 cells were plated in a 96-well dish in DMEM media containing 10% FBS and selective antibiotics (1µg/ml puromycin (P8833, Sigma-Aldrich) and/or 5µg/ml blasticidin (71002-676, VWR)), allowed to settle at room temperature for 20 minutes, then placed

in an Incucyte® S3 (Sartorius). Pictures were taken with a 10x magnification every 2 hours for 48 hours using a Standard scan. Confluency was determined using the Incucyte ZOOM software. Growth rate was calculated from % confluency using the Least Squares Fitting Method[56].

Soft Agar Colony Formation Assays

1% agar (BD Difco Agar Noble) was melted, cooled to 45°C, and mixed in equal volume with 2x Complete Media (2x Cell Culture Media (20 g/L DMEM/F12, Gibco #12400-016, 2 g/L sodium bicarbonate), 20% FBS, 2% Pen/Strep). 1.5 ml of mixture was pipetted into each well of a 6-well dish and allowed to set at room temperature for 30 minutes. Cells were trypsinized and quantified, and 50,000 cells were diluted in 3.75 ml 2x Complete Media. 0.6% agar was melted, cooled to 45°C, and mixed in equal volume with the cell dilution. 1.5 ml of mixture was plated to 4 replicate wells and allowed to cool at room temperature for 30 minutes. 1.5 ml of 1x Complete Media was added to the top of each well and cells were incubated at 37°C under standard cell culture conditions. Media was changed once every 5 days, and plates were incubated until colonies were visible by eye, approximately 3-4 weeks. Top media was replaced with 2 ml fresh 1x Complete Media and 100 µl 2 mg/ml Nitro Blue Tetrazolium (J60230, Thermo Fisher Scientific) was added. Plates were gently swirled to mix and incubated overnight at 37°C. Wells were imaged and ImageJ software was used to quantify colony count and size for each well.

Purification of METTL3/14

Suspension-adapted HEK293 cells (Freestyle™ 293-F cells, R790-07, Life Technologies) were grown as recommended in Freestyle™ 293 Expression Medium (12338026, Life Technologies,) sharking at 37°C in 5% CO_2. Cells were grown to a concentration of 3 x 10^6 cells/ml and diluted to 1 x 10^6 cells/ml in 50 ml 293F Freestyle Media 24 hours prior to transfection. Before transfection, cells were spun down and resuspended in 50 ml fresh 293F Freestyle Media at a concentration of 2.5 x 10^6 cells/ml. Expression plasmid (pcDNA3.1-FLAG-METTL3, pcDNA3.1-FLAG-METTL14) were added to the flask at a concentration of 1.5 µg, and flask was shaken in the incubator for 5 minutes. 9 µg/ml PEI was added to the flask and cells were returned to incubator. After 24 hours of growth, an additional 50 ml fresh 293F Freestyle Media was added and culture was supplemented with 2.2 mM VPA. Cells were harvested as two 50 ml pellets 72 hours after addition of VPA.

Cell pellets were resuspended in 1x Lysis Buffer (50 mM Tris pH 7.4, 150 mM Sodium Chloride, 1 mM EDTA, 1% TritonX-100, 1x Protease inhibitors) to obtain a concentration of 10^7 cells/ml and incubated for 20 minutes at 4°C with rotation. Cell lysate was clarified by centrifugation at 4°C, 12,000 x *g* for 15 minutes. Supernatant was transferred to a new tube and kept on ice. Anti-FLAG M2

affinity resin was equilibrated with 1x Lysis Buffer by washing 3 times. Equilibrated resin was resuspended in 1x Lysis Buffer and added to the tube containing the clarified lysate. Sample was incubated for 2 hours at 4°C with rotation. Resin was pelleted by centrifugation at 4°C, 500 x *g*. Supernatant was removed, and resin was washed 3 times with 1x Wash Buffer (50 mM Tris pH 7.4, 150 mM Sodium Chloride, 10% Glycerol, 1 mM Dithiothreitol) for 5 minutes each at 4°C with rotation. Sample was equilibrated to room temperature and resin was resuspended in 1x Wash Buffer containing 0.2 mg/ml 3xFLAG Peptide. Samples were incubated at room temperature for 10 minutes shaking at 1000 rpm, centrifuged for 2 minutes at 1000 x g, and supernatant was reserved (elution 1). Elution was repeated twice to obtain two additional elution samples (elution 2 and 3). Samples were analyzed by Coomassie to determine protein concentration and purity. Samples were aliquoted and stored at -80°C and thawed on ice prior to use in *in vitro* m6A methylation experiments.

***In vitro* m6A methylation and interaction assays**

Using PCR, we generated a DNA fragment for Domain 2 of wild-type (pTRE3G-HOTAIR, pAJ171) and A783U (pTRE3G-A783U_HOTAIR, pAJXXX) mutant HOTAIR using primers MB88 and MB89. A 5' T7 promoter and 3' RAT tag were added to the sequence via PCR with primers MB22 and MB94. *in vitro* transcription of the PCR templates was completed using the MEGAScript T7 Transcription Kit (AM1334, ThermoFisher Scientific) according to the manufacturer's instructions, and RNA was purified using the RNeasy Mini Kit (Qiagen 75106). 500 nM RNA was diluted in 1x Methyltransferase Buffer (20 mM Tris pH 7.5, 0.01% Triton-X 100, 1 mM DTT) in reactions containing 50 µM SAM and 500 nM purified METTL3/14 (+m6A) for 1 hour at room temperature. Control reactions contained no METTL3/14 (-m6A). RNA was purified using the RNeasy Mini Kit according to manufacturer's instructions.

To obtain FLAG-tagged YTHDC1 protein, 293 cells were transfected using Lipofectamine 2000 (11668030, ThermoFisher Scientific) with plasmid YTHDC1-FLAG and cell lysates were generated as previously described[24]. Dynabeads (M270, Invitrogen) were resuspended in high-quality dry Dimethylformamide at a concentration of 2 x 10^9 beads/ml. Dynabeads were stored at 4°C and equilibrated to room temperature prior to use. Dynabeads were washed in 0.1 M Sodium Phosphate Buffer (pH 7.4) and vortexed for 30 seconds. A second wash was repeated with vortexing and incubation at room temperature for 10 minutes with rotation. 1 mg/ml IgG solution was prepared by diluting rabbit IgG (15006, Sigma) in 0.1 M Sodium Phosphate Buffer. Washed beads were resuspended in 0.1 M Sodium Phosphate Buffer at a concentration of 3 x 10^9 beads/ml, and an equal volume of 1 mg/ml IgG was added. Samples were vortexed briefly and an equal volume of 3M Ammonium Sulfate was added and samples were mixed well. Samples were incubated at 37°C for 18-24 hours with rotation. Samples were washed once briefly with 0.1 M Sodium Phosphate Buffer, then twice with incubation at room temperature for 10 minutes with rotation. Samples were washed in Sodium Phosphate Buffer + 1% TritonX-100 at

37°C for 10 minutes with rotation. A quick wash with 0.1 M Sodium Phosphate Buffer was performed and followed by 4 washes in 0.1 M Citric Acid pH 3.1 at a concentration of 2 x 10^8 beads/ml at room temperature for 10 minutes with rotation. After a quick wash with 0.1 M Sodium Phosphate Buffer, beads were resuspended to 1 x 10^9 beads/ml in 1x PBS + 0.02% Sodium Azide and stored at 4°C prior to use.

800 ng of +/-m6A RNA was incubated with 150 ng PrA-PP7 fusion protein in HLB300 (20 mM Hepes pH 7.9, 300 mM sodium chloride, 2 mM magnesium chloride, 0.1% NP-40, 10% glycerol, 0.1 mM PMSF, 0.5 mM DTT). RNA was prebound to PP7 for 30 minutes at 25°C, 1350 rpm. 75 µl IgG-coupled Dynabeads were washed with HLB300 twice and resuspended in 250 µl HLB300. 50 µl beads were added to each tube of RNA-PP7 and samples were incubated 1 hour at 25°C, 1350 rpm. Beads were washed twice with HLB300 and resuspended in 80 µl Binding Buffer (10 mM Hepes pH 7.4, 150 mM potassium chloride, 3 mM magnesium chloride, 2 mM DTT, 0.5% NP-40, 10% glycerol, 1mM PMSF, 1x protease inhibitors) containing 80U RNase Inhibitor. 25 µg YTHDC1-FLAG containing lysate and 800 ng competitor RNA (IVT untagged HOTAIR D2) was added to each sample. Samples were incubated at 4°C for 2.5 hours on a rotor. Beads were washed 3 times with cold Wash Buffer (200 mM Tris-HCl pH 7.4, 200 mM sodium chloride, 2 mM magnesium Chloride, 1 mM DTT, 1x protease inhibitors) and resuspended in 1x SDS loading buffer. A 10% protein input sample was diluted in 1x SDS loading buffer. Samples were boiled 5 minutes at 95°C and supernatant transferred to a new tube. Half of each sample was loaded on a 10% acrylamide gel and Western Blot was performed using anti-FLAG antibody.

Fractionation

Cells were grown in 15 cm dishes to 70-90% confluency. Cells were released with Trypsin (Corning), washed once with 1x PBS containing 1 mM EDTA, and split into two volumes. 1/4 of the sample was harvested in TRIzol and RNA isolated with RNeasy kit for the input RNA sample. The remaining ¾ of the sample was fractionated into cytoplasmic, nucleoplasmic, and chromatin-associated samples. Cells were lysed in cold Cell Lysis Buffer (10 mM Tris-HCl pH 7.5, 0.15% NP-40, 150 mM Sodium Chloride) containing RNase inhibitors for 5 minutes on ice. Lysate was layered onto 2.5 volumes of Sucrose Cushion (10mM Tris-HCl pH7.5, 150 mM Sodium Chloride, 24% Sucrose) containing RNase inhibitors. Samples were centrifuged for 10 minutes at 17,000*xg* at 4°C. Supernatant was collected (Cytoplasmic sample). Pellet was rinsed with 1x PBS containing 1 mM EDTA and resuspended in cold Glycerol Buffer (20 mM Tris-HCl pH 7.9, 75 mM Sodium Chloride, 0.5 mM EDTA, 0.85 mM DTT, 0.125 mM PMSF, 50% Glycerol) containing RNase inhibitors. An equal volume of cold Nuclei Lysis Buffer (10 mM HEPES pH 7.6, 1 mM DTT, 7.5 mM Magnesium Chloride, 0.2 mM EDTA, 0.3 M Sodium Chloride, 1M Urea, 1% NP-40) was added and sample was briefly vortexed twice for 2 seconds. Samples were incubated on ice 2 minutes and centrifuged for 2 minutes at 17,000*xg* at 4°C. Supernatant was collected (Nucleoplasmic sample). The

remaining pellet was resuspended in 1x PBS containing 1 mM EDTA (Chromatin-associated sample). Each sample was subjected to TURBO DNase digestion at 37°C for 30 minutes in 1x TURBO Buffer and 10 U TURBO for cytoplasmic and nucleoplasmic samples, or 40U TURBO for chromatin-associated sample. Reactions were quenched with 10mM EDTA and 3 volumes of TRIzol-LS was added. RNA isolation was performed as recommended by manufacturer. Samples were quantified by nanodrop to determine RNA concentration and ran on a 2% agarose gel to confirm RNA integrity. qRT-PCR was performed on 2 µg of RNA and normalized to RNA recovery, input values, and GAPDH.

siRNA Transfection

Silencer Select siRNAs were obtained from ThermoFisher targeting YTHDC1 (n372360, n372361, n372362) or Negative Controls (4390843, 4390846) and transfected into 293 cell lines using Lipofectamine RNAiMAX Transfection Reagent (13778030, ThermoFisher). Transfections were performed in a 24-well plate with 5 pmol of siRNA and 1.5 µl RNAiMAX Transfection reagent per well. Cells were harvested 24 hours after transfections and analyzed by Luciferase Assay and qRT-PCR.

Luciferase Assay

Analysis of luciferase activity was performed using the Luciferase Assay System (E1500, Promega). Cells were washed with 1x PBS and lysed in 100 µl 1x Cell Culture Lysis Reagent. Cells were scraped from bottom of dish and suspension was transferred to a new tube. Lysates were frozen and thawed prior to luciferase assay to ensure complete lysis. Luciferase assays were performed on 20 µl of lysate or 1x Cell Culture Lysis Reagent in 96 well plates on the GloMax-Multi Detection System (TM297, Promega). 100 µl Luciferase Assay Reagent was added to wells, mixed, and light production measured. Measurements were performed in 3 technical replicates for each biological replicate. Luciferase activity was normalized to protein concentration of samples.

Acknowledgements

This work was funded by the NIH (R35GM119575 (AMJ), R01CA187733 (JKR), T32CA190216 (AMP), T32GM008730 (JTR), F32CA239436 (MMW), and NCI Cancer Center Support Grant P30CA046934 to the University of Colorado Cancer Center), a Department of Defense Breast Cancer Research Program Breakthrough Fellowship Award BC170270 (AMP), and an RNA Bioscience Initiative Grant. We thank Maggie M. Balas for figure advice and preparation, Rafael Margueron for providing cell lines used in this study, Chuan He for providing METTL3 and METTL14 expression plasmids, and John Rinn, Suja Jagannathan, and Neelanjan Mukherjee for their suggestions on the manuscript.

Author Contributions

AMP, JTR, JKR, MMW, and AMJ designed research; AMP, JTR, MC, MK performed experiments; AMP and JTR analyzed data; and AMP, JKR, and AMJ wrote the paper.

References

1. Long, Y., Wang, X., Youmans, D. T. & Cech, T. R. How do lncRNAs regulate transcription? *Sci. Adv.* **3**, eaao2110 (2017).
2. Esteller, M. Non-coding RNAs in human disease. *Nat. Rev. Genet.* **12**, 861–874 (2011).
3. Balas, M. M. & Johnson, A. M. Exploring the mechanisms behind long noncoding RNAs and cancer. *Non-coding RNA Res.* **3**, 108–117 (2018).
4. Shi, H., Wei, J. & He, C. Where, When, and How: Context-Dependent Functions of RNA Methylation Writers, Readers, and Erasers. *Mol. Cell* **74**, 640–650 (2019).
5. Coker, H. *et al.* The role of the Xist 5' m6A region and RBM15 in X chromosome inactivation. *Wellcome open Res.* **5**, 31 (2020).
6. Patil, D. P. *et al.* m6A RNA methylation promotes XIST-mediated transcriptional repression. *Nature* **537**, 1–25 (2016).
7. Zaccara, S., Ries, R. J. & Jaffrey, S. R. Reading, writing and erasing mRNA methylation. *Nat. Rev. Mol. Cell Biol.* **20**, 608–624 (2019).
8. Nesterova, T. B. *et al.* Systematic allelic analysis defines the interplay of key pathways in X chromosome inactivation. *Nat. Commun.* **10**, 3129 (2019).
9. Liu, J. *et al.* N6-methyladenosine of chromosome-associated regulatory RNA regulates chromatin state and transcription. *Science (80-.).* **367**, 580 LP – 586 (2020).
10. Coker, H., Wei, G. & Brockdorff, N. m6A modification of non-coding RNA and the control of mammalian gene expression. *Biochim. Biophys. acta. Gene Regul. Mech.* **1862**, 310–318 (2019).
11. Rinn, J. L. *et al.* Functional Demarcation of Active and Silent Chromatin Domains in Human HOX Loci by Noncoding RNAs. *Cell* **129**, 1311–1323 (2007).
12. Gupta, R. a *et al.* Long non-coding RNA HOTAIR reprograms chromatin state to promote cancer metastasis. *Nature* **464**, 1071–6 (2010).
13. Wu, Y. *et al.* Long non-coding RNA HOTAIR promotes tumor cell invasion and metastasis by recruiting EZH2 and repressing E-cadherin in oral squamous cell carcinoma. *Int. J. Oncol.* **46**, 2586–2594 (2015).
14. Tsai, M.-C. *et al.* Long noncoding RNA as modular scaffold of histone modification complexes. *Science* **329**, 689–93 (2010).
15. Hajjari, M. & Salavaty, A. HOTAIR: an oncogenic long non-coding RNA in different cancers. *Cancer Biol. Med.* **12**, 1–9 (2015).
16. Portoso, M. *et al.* PRC2 is dispensable for HOTAIR-mediated transcriptional repression. *EMBO J.* (2017). doi:10.15252/embj.201695335

17. Cifuentes-Rojas, C., Hernandez, A. J., Sarma, K. & Lee, J. T. Regulatory Interactions between RNA and Polycomb Repressive Complex 2. *Mol. Cell* **55**, 171–185 (2014).

18. Davidovich, C., Zheng, L., Goodrich, K. J. & Cech, T. R. Promiscuous RNA binding by Polycomb repressive complex 2. *Nat. Struct. Mol. Biol.* **20**, 1250–1257 (2013).

19. Beltran, M. *et al.* The interaction of PRC2 with RNA or chromatin s mutually antagonistic. *Genome Res.* **26**, 896–907 (2016).

20. Wu, X., Sang, L. & Gong, Y. N6-methyladenine RNA modification and cancers. *Am. J. Cancer Res.* **8**, 1957–1966 (2018).

21. Zhang, C. *et al.* Hypoxia-inducible factors regulate pluripotency factor expression by ZNF217- and ALKBH5-mediated modulation of RNA methylation in breast cancer cells. *Oncotarget* **7**, 64527–64542 (2016).

22. Niu, Y. *et al.* RNA N6-methyladenosine demethylase FTO promotes breast tumor progression through inhibiting BNIP3. *Mol. Cancer* **18**, 46 (2019).

23. Zhang, J. X. *et al.* HOTAIR, a cell cycle-associated long noncoding RNA and a strong predictor of survival, is preferentially expressed in classical and mesenchymal glioma. *Neuro. Oncol.* **15**, 1595–1603 (2013).

24. Meredith, E. K., Balas, M. M., Sindy, K., Haislop, K. & Johnson, A. M. An RNA matchmaker protein regulates the activity of the long noncoding RNA HOTAIR. *RNA* 1–16 (2016). doi:10.1261/rna.055830.115

25. Han, Y. *et al.* CVm6A: A Visualization and Exploration Database for m(6)As in Cell Lines. *Cells* **8**, (2019).

26. Roberts, J. T., Porman, A. M. & Johnson, A. M. Identification of m6A residues at single-nucleotide resolution using eCLIP and an accessible custom analysis pipeline. *bioRxiv* 2020.03.11.986174 (2020). doi:10.1101/2020.03.11.986174

27. Somarowthu, S. *et al.* HOTAIR forms an intricate and modular secondary structure. *Mol. Cell* **58**, 353–361 (2015).

28. Akiyama, M., Sato, K. & Sakakibara, Y. A max-margin training of RNA secondary structure prediction integrated with the thermodynamic model. *J. Bioinform. Comput. Biol.* **16**, 1840025 (2018).

29. Arshi A, Raeisi F, Mahmoudi E, Mohajerani F, Kabiri H, Fazel R, Zabihian-Langeroudi M, J. A. A comparative study of HOTAIR expression in breast cancer patient tissues and cell lines. *Cell J* **22**, 178–184 (2020).

30. Alarcon, C. R. *et al.* HNRNPA2B1 Is a Mediator of m(6)A-Dependent Nuclear RNA Processing Events. *Cell* **162**, 1299–1308 (2015).

31. Wu, Y. *et al.* m(6)A-induced lncRNA RP11 triggers the dissemination of colorectal cancer cells via upregulation of Zeb1. *Mol. Cancer* **18**, 87 (2019).

32. Nguyen, E. D., Balas, M. M., Griffin, A. M., Roberts, J. T. & Johnson, A. M. Global profiling of hnRNP A2/B1-RNA binding on chromatin highlights LncRNA interactions. *RNA Biol.* **15**, 901–913 (2018).

33. Tang, Z., Kang, B., Li, C., Chen, T. & Zhang, Z. GEPIA2: an enhanced web server for large-scale expression profiling and interactive analysis. *Nucleic Acids Res.* **47**, W556–W560 (2019).

34. Gyorffy, B. *et al.* An online survival analysis tool to rapidly assess the effect of 22,277 genes on breast cancer prognosis using microarray data of 1,809 patients. *Breast Cancer Res. Treat.* **123**, 725–731 (2010).

35. Chandrashekar, D. S. *et al.* UALCAN: A Portal for Facilitating Tumor Subgroup Gene Expression and Survival Analyses. *Neoplasia* **19**, 649–658 (2017).

36. Rezaul, K. *et al.* Differential protein expression profiles in estrogen receptor-positive and -negative breast cancer tissues using label-free quantitative proteomics. *Genes Cancer* **1**, 251–271 (2010).

37. Liu, J. *et al.* A METTL3-METTL14 complex mediates mammalian nuclear RNA N6-adenosine methylation. *Nat. Chem. Biol.*

10, 93–5 (2014).

38. Cowley, M. J. *et al.* PINA v2.0: mining interactome modules. *Nucleic Acids Res.* **40**, D862–D865 (2012).

39. Haque, N. & Oberdoerffer, S. Chromatin and splicing. *Methods Mol. Biol.* **1126**, 97–113 (2014).

40. Brody, Y. & Shav-Tal, Y. Transcription and splicing: when the twain meet. *Transcription* **2**, 216–220 (2011).

41. Slobodin, B. *et al.* Transcription Impacts the Efficiency of mRNA Translation via Co-transcriptional N6-adenosine Methylation. *Cell* **169**, 326-337.e12 (2017).

42. Ke, S. *et al.* m(6)A mRNA modifications are deposited in nascent pre-mRNA and are not required for splicing but do specify cytoplasmic turnover. *Genes Dev.* **31**, 990–1006 (2017).

43. Weighardt, F., Biamonti, G. & Riva, S. The roles of heterogeneous nuclear ribonucleoproteins (hnRNP) in RNA metabolism. *BioEssays news Rev. Mol. Cell. Dev. Biol.* **18**, 747–756 (1996).

44. Xiao, W. *et al.* Nuclear m(6)A Reader YTHDC1 Regulates mRNA Splicing. *Mol. Cell* **61**, 507–519 (2016).

45. Liang, S. *et al.* Human cytomegalovirus ie2 affects the migration of glioblastoma by mediating the different splicing patterns of RON through hnRNP A2B1. *Neuroreport* **30**, 805–811 (2019).

46. Alarcón, C. R. *et al.* HNRNPA2B1 Is a Mediator of m(6)A-Dependent Nuclear RNA Processing Events. *Cell* **162**, 1299–308 (2015).

47. Hartmann, A. M., Nayler, O., Schwaiger, F. W., Obermeier, A. & Stamm, S. The interaction and colocalization of Sam68 with the splicing-associated factor YT521-B in nuclear dots is regulated by the Src family kinase p59(fyn). *Mol. Biol. Cell* **10**, 3909–3926 (1999).

48. Ries, R. J. *et al.* m6A enhances the phase separation potential of mRNA. *Nature* **571**, 424–428 (2019).

49. Strom, A. R. *et al.* Phase separation drives heterochromatin domain formation. *Nature* **547**, 241 (2017).

50. Roundtree, I. A. *et al.* YTHDC1 mediates nuclear export of N(6)-methyladenosine methylated mRNAs. *Elife* **6**, (2017).

51. Liu, N. *et al.* Probing N6-methyladenosine RNA modification status at single nucleotide resolution in mRNA and long noncoding RNA. *RNA* **19**, 1848–1856 (2013).

52. Zheng, Q. *et al.* Long noncoding RNA MEG3 suppresses liver cancer cells growth through inhibiting β-catenin by activating PKM2 and inactivating PTEN. *Cell Death Dis.* **9**, 253 (2018).

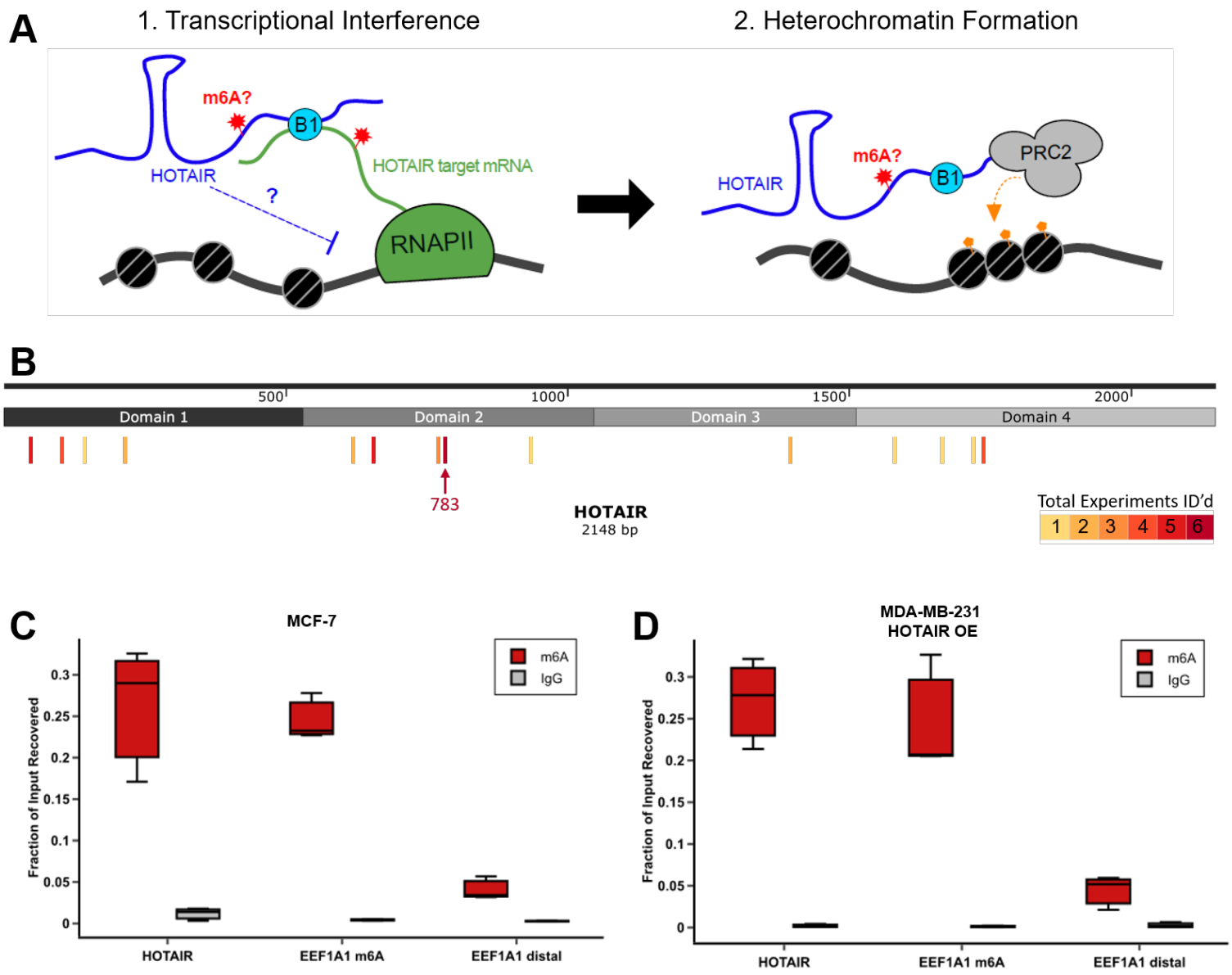

Figure 1. LncRNA HOTAIR is m6A modified. A) General model for HOTAIR mechanism. HOTAIR is initially recruited to its target loci via RNA-RNA interactions with its mRNA targets which is mediated by hnRNP B1. HOTAIR association with chromatin induces transcriptional interference via an unknown mechanism, promoting heterochromatin formation by PRC2 through H3K27me3. This paper investigates the role of m6A on HOTAIR. **B)** m6A sites detected in HOTAIR-expressing cells in 6 experiments (yellow to red scale of increasing occurrences). m6A site 783 (dark red, arrow) was detected in every experiment except where it was mutated. **C-D)** m6A RNA immunoprecipitation performed with an m6A antibody or IgG control in MCF-7 breast cancer cells (C) or MDA-MB-231 breast cancer cells with transgenic overexpression of HOTAIR (D). An m6A modified region in EEF1A1 (EEF1A1 m6A) is a positive control, while a distal region in EEF1A1 that is not m6A modified (EEF1A1 distal) serves as a negative control.

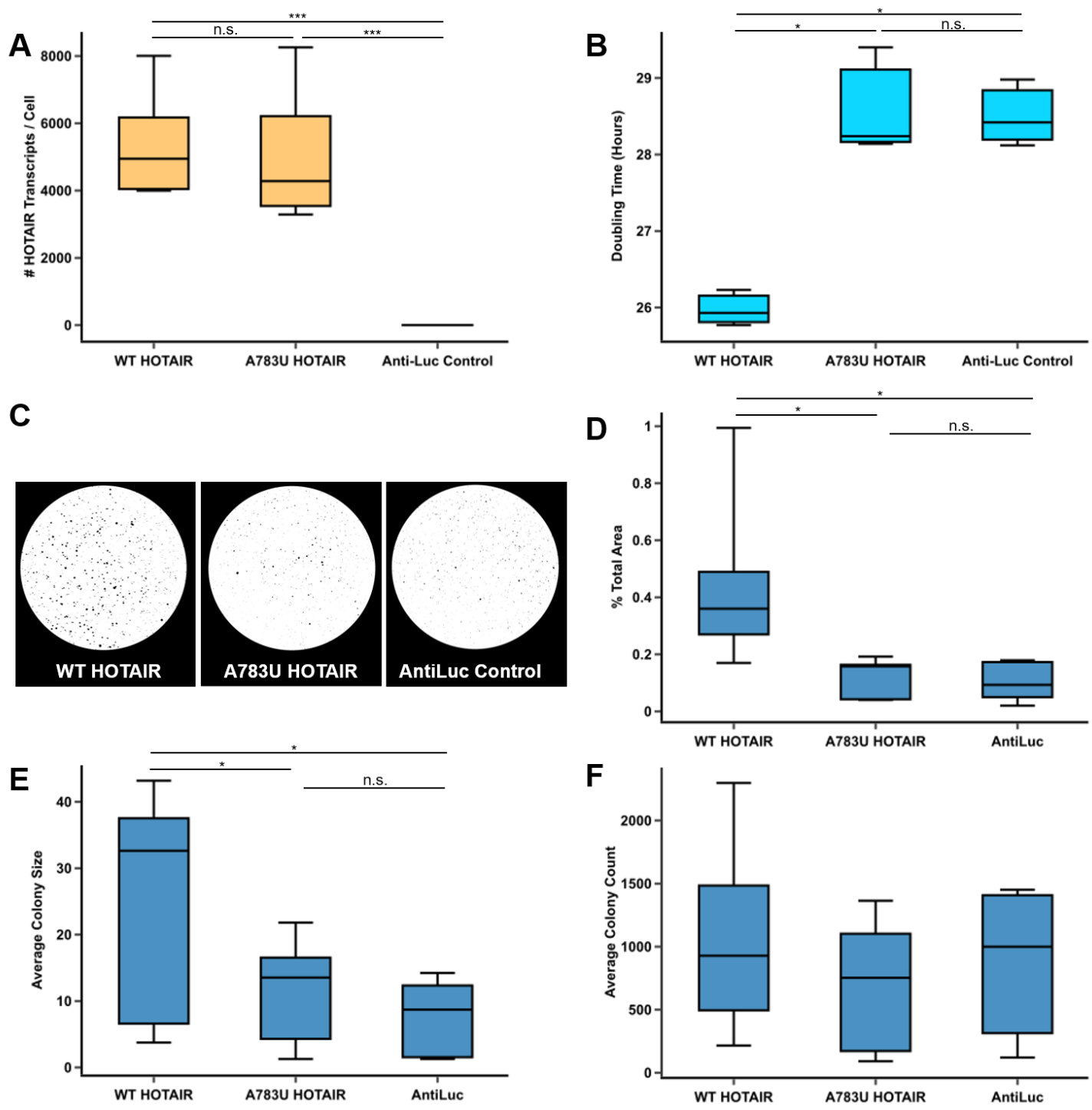

Figure 2. m6A site 783 mediates the ability of HOTAIR to enhance breast cancer growth. A) Relative HOTAIR expression in MDA-MB-231 cells overexpressing WT HOTAIR, A783U HOTAIR, or an Anti-Luciferase control RNA. *** $p<0.001$ **B)** Doubling time of MDA-MB-231 overexpression cell lines described in (A). * $p<0.05$ **C)** Example images of soft agar colony formation assays of MDA-MB-231 overexpression cell lines. **D-F)** Quantification of % total area (D), average colony size (E), and average colony count (F) of soft agar assays. 4 replicates were performed. * $p<0.05$

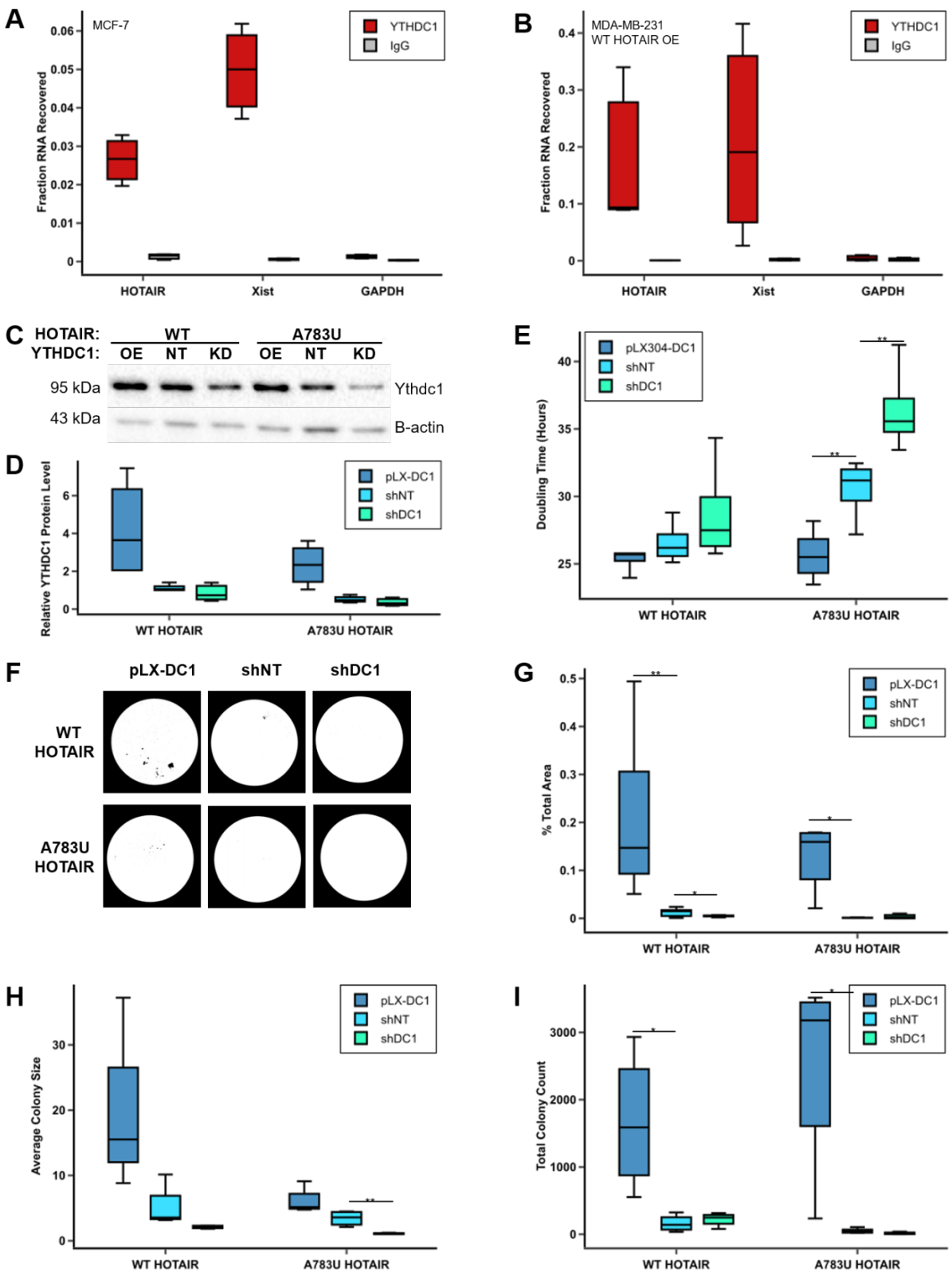

Figure 3. YTHDC1 interacts with HOTAIR and enables HOTAIR-mediated breast cancer growth. A-B) YTHDC1 RIP performed in MCF-7 cells (A) or MDA-MB-231 cells overexpressing transgenic HOTAIR (B). **C)** Western blot results of YTHDC1 protein levels in pLX-DC1 overexpression, shNT control, and shDC1 knockdown MDA-MB-231 cell lines expressing WT or A783U HOTAIR. **D)**

Quantification of 3 replicates of (C). **E)** Doubling time of MDA-MB-231 cells containing WT or A783U HOTAIR and overexpression or knockdown of YTHDC1. **F)** Examples of soft agar colony formation assays on MDA-MB-231 cell lines. **G-H)** Quantification of total area (G), average colony size (H), and total colony count (I) of soft agar colony formation assays on MDA-MB-231 cell lines. * $p < 0.05$, ** $p < 0.01$

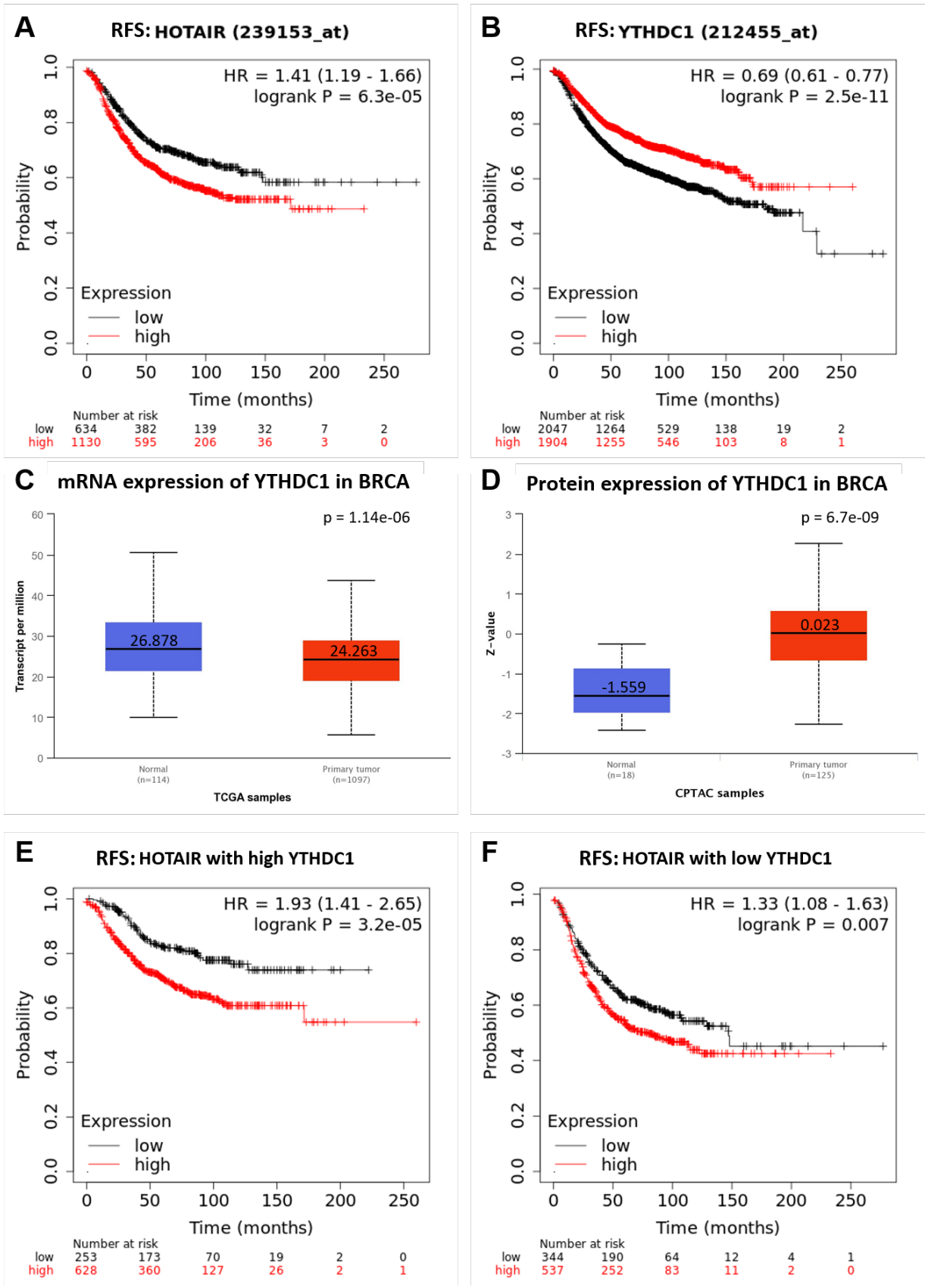

Figure 4. *YTHDC1* and *HOTAIR* in breast cancers. A-B) Kaplan-Meier curves for recurrence-free survival of breast cancer patients with high or low expression of A) *YTHDC1* or B) *HOTAIR* generated using Kaplan-Meier Plotter[34]. **C-D)** Expression of YTHDC1 C)

mRNA and D) protein in normal breast tissue versus breast cancers generated with UALCAN[35]. **E-F)** Recurrence-free survival curves for breast cancer patients examining effect of HOTAIR on the background of either E) high or F) low *YTHDC1* levels, generated with Kaplan-Meier Plotter[34].

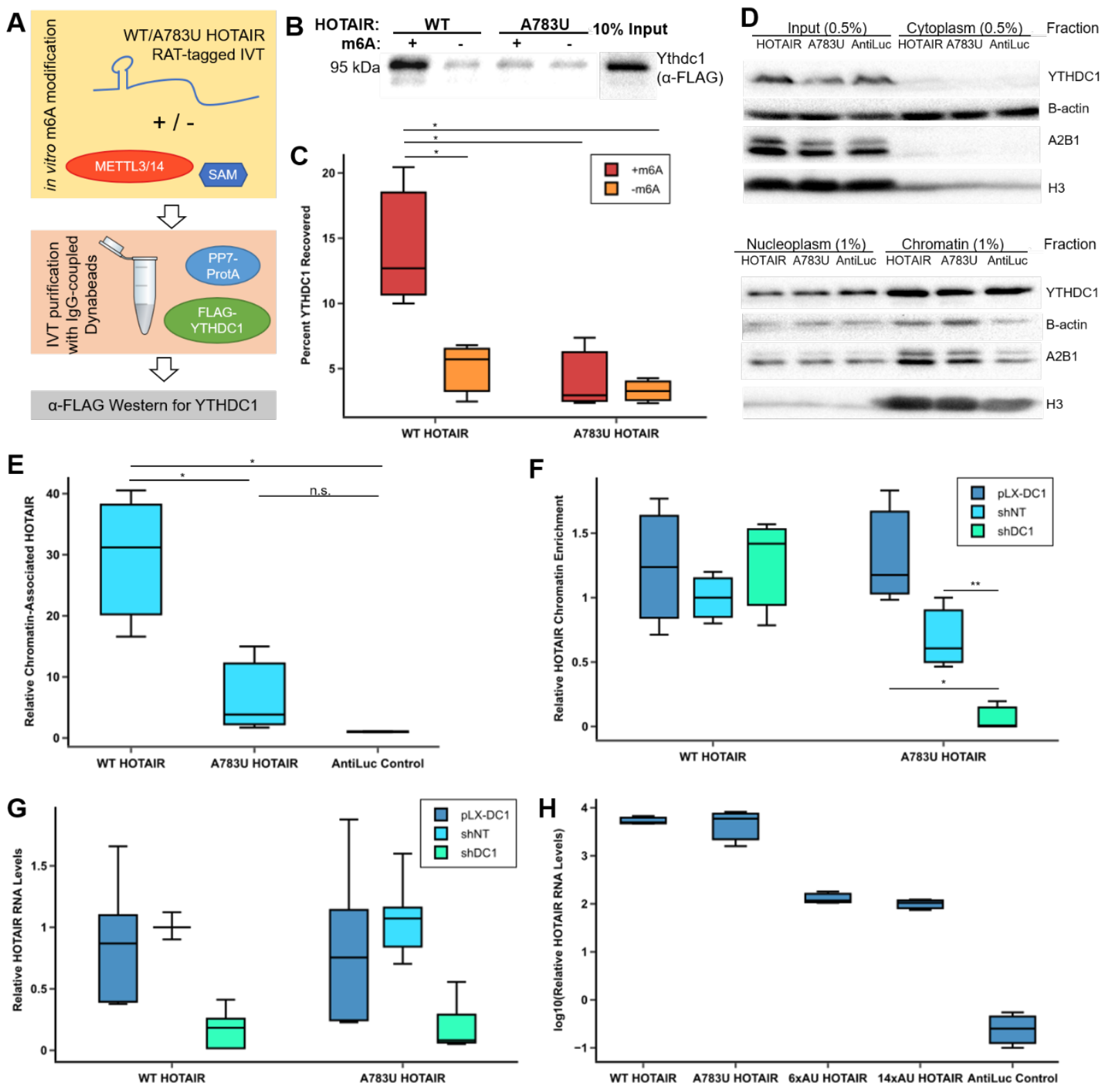

Figure 5. HOTAIR m6A site 783 mediates interaction with YTHDC1 and chromatin association. A) Schematic of YTHDC1 pulldown experiment with m6A-modified WT and A783U HOTAIR. PP7-tagged domain 2 of WT or A783U HOTAIR was *in vitro* transcribed and m6A modified with purified METTL3/14. RNA was bound to PP7-Protein A, cellular extract containing FLAG-tagged YTHDC1 was added, and a pulldown was performed with IgG-coupled Dynabeads. Amount of FLAG-YTHDC1 bound was assessed

by Western blot. **B)** Anti-FLAG Western blot of pulldown experiment outlined in (A). **C)** Quantification of anti-FLAG Western blots from 3 replicates. **D)** Western blot performed on fractionation of MDA-MB-231 cell lines overexpressing WT or A783U HOTAIR or Antisense-Luciferase. **E)** qRT-PCR was performed on fractionated RNA samples from MDA-MB-231 cells containing overexpression of WT HOTAIR, A783U HOTAIR, or an Anti-Luc control, and chromatin enrichment was calculated by determining the relative chromatin-associated RNA to input and normalizing to GAPDH levels and MDA-MB-231 Anti-Luc control cells. **F)** Chromatin enrichment was calculated similarly as in (D) in MDA-MB-231 cell lines expressing WT or A783U HOTAIR with knockdown or overexpression of YTHDC1. * $p < 0.05$, ** $p < 0.01$ **G)** qRT-PCR of *HOTAIR* RNA levels in MDA-MB-231 cell lines overexpressing WT or A783U HOTAIR containing overexpression or knockdown of YTHDC1. **H)** qRT-PCR of *HOTAIR* RNA levels in MDA-MB-231 cell lines expressing WT, A783U, 6xAU, or 14xAU HOTAIR or an AntiLuc control.

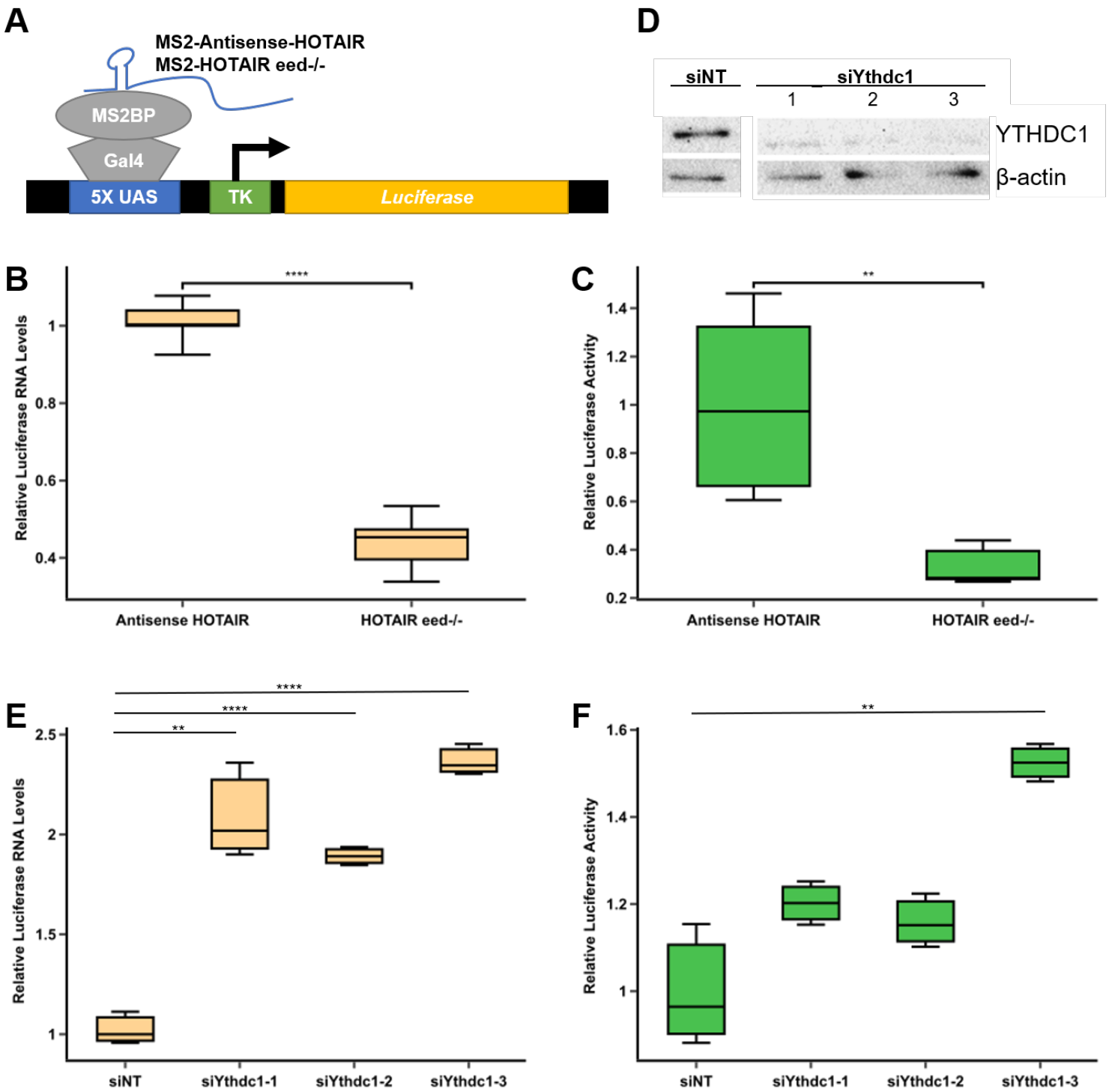

Figure 6. YTHDC1 mediates transcriptional repression by HOTAIR. A) Schematic of 293T cells containing MS2-Antisense-HOTAIR or MS2-HOTAIR tethered upstream of a luciferase reporter. MS2-HOTAIR tethered cells also contain a deletion of *EED*, a subunit of PRC2 that is critical for H3K27 methylation. B-C) Relative luciferase RNA levels (B) and relative luciferase activity (C) in MS2-Antisense HOTAIR or MS2-HOTAIR eed-/- cell lines. D) Western blot of YTHDC1 in MS3-HOTAIR eed-/- 293T reporter cells transfected with

non-targeting siRNA or 3 different siRNAs targeting YTHDC1. E-F) Relative luciferase RNA levels (E) and relative luciferase activity (F) of HOTAIR-tethered eed-/- cells transfected with a non-targeting siRNA or 3 different siRNAs against YTHDC1.

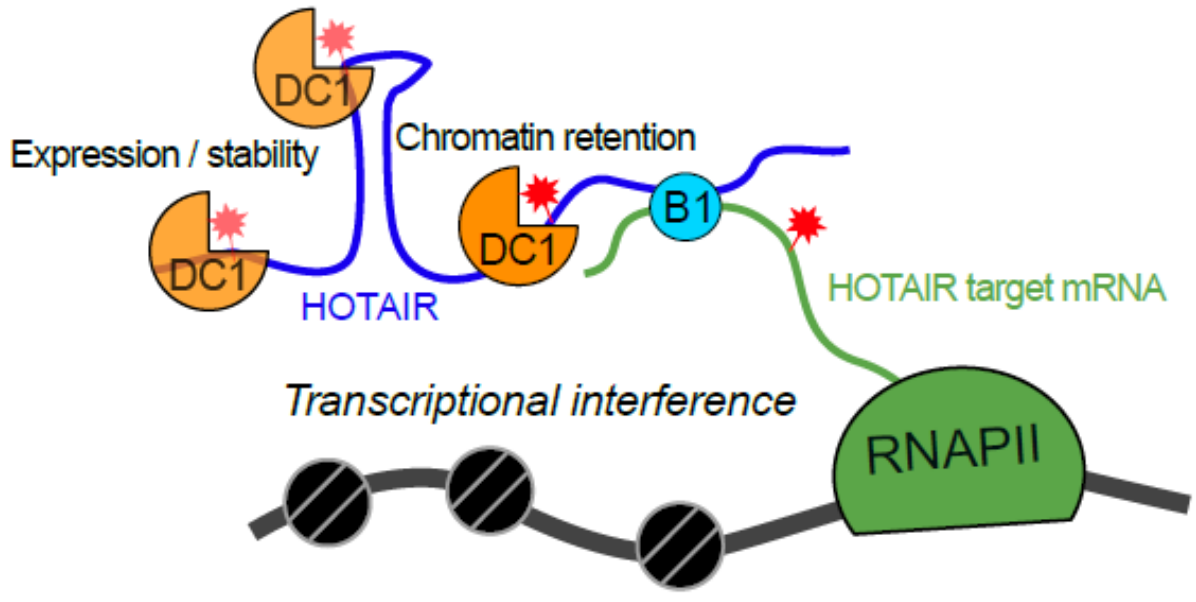

Figure 7. Model of m6A and YTHDC1 effects on HOTAIR. The main function of YTHDC1 occurs via interaction with m6A783 in HOTAIR and mediates chromatin retention of HOTAIR to induce transcriptional interference of its target genes, promoting breast cancer growth. YTHDC1 also interacts with other m6A sites within HOTAIR and may mediate its high expression levels and/or stability.